

AI for the Routine, Humans for the Complex: Accuracy-Driven Data Labelling with Mixed Integer Linear Programming

Mohammad Hossein Amini, Mehrdad Sabetzadeh, and Shiva Nejati

Abstract—The scarcity of accurately labelled data remains a major challenge in deep learning (DL). Many DL approaches rely on semi-supervised methods, which focus on constructing large datasets that require only a minimal amount of human-labelled data. Since DL training algorithms can tolerate moderate label noise, it has generally been acceptable for the accuracy of labels in large training datasets to fall well short of a perfect 100%. However, when it comes to testing DL models, achieving high label accuracy – as close to 100% as possible – is paramount for reliable verification. In this article, we introduce OPAL, a human-assisted labelling method that can be configured to target a desired accuracy level while minimizing the manual effort required for labelling. The main contribution of OPAL is a mixed-integer linear programming (MILP) formulation that minimizes labelling effort subject to a specified accuracy target. To evaluate OPAL, we instantiate it for two tasks in the context of testing vision systems: automatic labelling of test data and automated validation of test data. Our evaluation, based on more than 2500 experiments performed on seven datasets, comparing OPAL with eight baseline methods, shows that OPAL, relying on its MILP formulation, achieves an average accuracy of 98.8%, just 1.2% below perfect accuracy, while cutting manual labelling by more than half. Further, OPAL significantly outperforms automated labelling baselines in labelling accuracy across all seven datasets, with large effect sizes, when all methods are provided with the same manual-labelling budget. For automated test-input validation, on average, OPAL reduces manual effort by 28.8% while achieving 4.5% higher accuracy than the state-of-the-art test-input validation baselines. Finally, we show that augmenting OPAL with an active learning loop leads to an additional 4.5% reduction in required manual labelling, without compromising accuracy.

Index Terms—Testing Deep Learning Systems, Vision-based Systems, Test-Input Labelling, Test-input Validation, Constrained Optimization Problems, Mixed-Integer Linear Programming (MILP), Supervised Learning, Pseudo Labelling, Active Learning

I. INTRODUCTION

Deep learning (DL) has become a cornerstone for numerous advanced applications, enabling the automation of complex tasks such as anomaly detection, object recognition, and semantic segmentation. Since DL is inherently data-driven, accurately testing and verifying DL systems necessitates large and diverse test sets. To address this need, researchers have developed a variety of synthetic test-input generation methods [1]–[6]. For example, a common approach for testing vision-based systems is to generate synthetic images, either by

perturbing existing images [1], [4], [7] or by using generative models [2], [6]. However, recent research indicates that these methods frequently produce images where the original or intended labels are not preserved, requiring manual review and relabelling [3], [4], [8]. It is therefore important to find ways to reduce the effort required for manual labelling.

Both supervised and semi-supervised learning have been explored to reduce the effort required for labelling large volumes of data, such as synthetic or web-crawled datasets [9]–[11]. Existing methods developed for this purpose typically use pretrained DL classifiers to generate provisional labels for unlabelled data. This provisionally labelled data is then merged – either fully or selectively – with the manually labelled data, usually for re-training or fine-tuning [9], [11]. This process can considerably decrease reliance on manual labelling. Nevertheless, existing methods pay little attention to the accuracy of the automatically generated labels. This is because DL training algorithms often tolerate moderate levels of labelling errors – around 10%, according to existing studies [12], [13] – without major compromises in accuracy, particularly when the training sets are large.

In contrast, when it comes to testing DL systems, it is essential that the test sets used be highly accurate to ensure reliable testing results [14], [15]. Even a small number of mislabelled elements in a test set can lead to either inflated or deflated measured accuracy of the system under test. Inflated accuracy can create a false sense of confidence in the system’s trustworthiness, making it more likely that genuine faults will be overlooked, potentially leading to critical failures. Deflated accuracy, on the other hand, misrepresents trustworthiness by generating spurious errors, i.e., false issues caused by label inaccuracies rather than actual system flaws. Such errors waste time and effort by prompting investigations into non-existent issues and can also potentially divert attention from identifying and resolving genuine faults.

Reliable testing requires *near-perfect* test-set accuracy and *minimal human effort*. Yet, the machine learning (ML) community has largely overlooked this issue, since, as stated above, ML training is generally tolerant of labelling errors. The challenge, instead, reflects concerns more familiar to software engineering, where a central goal is to construct high-accuracy test sets while keeping associated costs in check.

We therefore argue that data labelling should be approached as an *accuracy-driven* process, in which explicit control is provided over the desired accuracy threshold, and effort is optimized subject to this threshold: for test sets, the goal would

M. H. Amini, M. Sabetzadeh, and S. Nejati are with the University of Ottawa, Canada. E-mail: {mh.amini, m.sabetzadeh, snejati}@uottawa.ca

typically be to achieve near-perfect label accuracy, and effort needs to be optimized subject to this goal, whereas for training sets, effort should be optimized according to a more relaxed criterion – namely, ensuring that the prevalence of mislabelling remains within the tolerance margin of the training algorithms.

In this article, we introduce OPAL, an effort-**O**ptimized Accuracy-driven data **L**abelling method. OPAL aims to meet or exceed a specified accuracy target with the least possible human effort. To do so, OPAL identifies difficult cases that classifiers cannot confidently label, directing them to humans for handling, while routine cases are automatically labelled by classifiers. OPAL relies on the predicted labels and prediction confidences obtained from a set of pretrained classifiers. It then uses an optimization solver to determine when the classifiers’ confidence levels are high enough to bypass manual labelling. The main novelty of OPAL is to formulate the optimization problem of minimizing human labelling effort under a specified accuracy threshold as a *mixed-integer linear program (MILP)* [16], [17] and to solve it efficiently.

Given the critical importance of labelling accuracy in testing, we evaluate OPAL for two tasks pertinent to testing vision-based systems: (1) automated test-data labelling, and (2) automated test-data validation [3], [4], [8]. Automated test-data labelling is about generating accurate labels for individual test images, while automated test-data validation is about determining whether a transformed image is an acceptable and valid alteration of its corresponding original image. We apply OPAL to seven image datasets: four real-world benchmarks and three synthetic datasets. We instantiate OPAL using a set of three widely used DL classifiers: VGG [18], ResNet [19], and ViT [20]. These represent complementary state-of-the-art DL architectures for vision-based systems: VGG is a convolutional neural network (CNN), ResNet extends CNNs with residual connections, and ViT employs transformers. In our experiments, we use versions of these classifiers pretrained on the ImageNet [21] dataset, which is not part of any of our seven evaluation datasets.

We compare OPAL with eight baselines. Four are state-of-the-art supervised or semi-supervised automated data-labelling techniques [11] from the ML and DL literature implemented with VGG, ResNet, and ViT backbones [18]–[20]. The other four are automated data-validation approaches taken from the software engineering literature, specifically from software testing [3], [4], [8]. Our evaluation relies on standard metrics: labelling accuracy and the amount of manual effort required. To assess OPAL for data labelling we use all seven of our datasets; to assess it for data validation we use the three datasets from the software engineering literature that contain both the original images and their transformed variants, making them suitable for the data-validation use case.

Our results obtained from more than 2500 experiments show that, across seven diverse datasets, when OPAL is configured to target 100% accuracy, it achieves an average accuracy of 98.8%, just 1.2% below perfect accuracy, while requiring 44.4% manual effort, effectively cutting manual labelling by more than half. Further, OPAL significantly outperforms the supervised and semi-supervised baselines in labelling accuracy for all seven datasets with large effect sizes. Under the same

manual labelling effort required by OPAL to achieve an average accuracy of 98.8%, none of the baselines exceed an average accuracy of 95.3%. For automated test-input validation, on average, OPAL reduces manual effort by 28.8% while achieving 4.5% higher accuracy than the four state-of-the-art test-input validation baselines [3], [4], [8]. Statistical tests confirm that both the reduction in manual effort and the improvement in accuracy are statistically significant, with a large effect size for manual effort reduction across all datasets and medium to large effect sizes for accuracy improvement across all datasets. We further show that incorporating an active-learning loop into OPAL reduces the required manual labelling by an additional 4.5% without compromising accuracy. Finally, OPAL has practical execution time. Specifically, our results indicate that OPAL’s main contribution – its MILP-based optimization step – is highly efficient, averaging only 24 seconds per dataset. This accounts for approximately 3% of the total execution time and is the only additional computational overhead compared to baselines that do not use accuracy-driven effort minimization.

II. OPAL AT A GLANCE

This section outlines OPAL and its novelty and significance.

Overview. Given an unlabelled dataset D and a set of pretrained classifiers, OPAL assigns a label to each element $e \in D$ automatically if all classifiers agree on the same label with high confidence; otherwise, e is labelled manually. The ultimate goal of OPAL, expressed as a constrained optimization problem below, is to *minimize the amount of manual labelling required while ensuring that the labelling accuracy meets or exceeds a threshold α* :

$$\begin{array}{ll} \text{minimize} & \text{Manual Effort} & (*) \\ \text{subject to} & \text{Accuracy} \geq \alpha \end{array}$$

The above constrained optimization problem computes the decision variables that determine when the classifiers’ confidence levels are sufficiently high to bypass manual labelling. However, computing these decision variables for a given dataset requires access to ground-truth labels for the dataset. Without ground-truth labels, one cannot measure the accuracy of the classifiers’ predictions and cannot ensure the $\text{Accuracy} \geq \alpha$ constraint.

Hence, OPAL selects a small subset $D_o \subset D$, referred to as the *optimization* subset, and obtains its ground-truth labels through manual labelling. It then solves problem (*) on D_o to determine the classifiers’ confidence levels that minimize manual labelling while ensuring classification accuracy meets or exceeds α for D_o . Next, OPAL applies these classifiers’ confidence levels to label the remaining unlabelled elements in D . Specifically, when all classifiers agree on a label for an unlabelled element $e \in D$ and their confidence meets or exceeds the levels derived from solving problem (*), e is labelled automatically; otherwise, it is labelled manually.

Because OPAL solves problem (*) only for the manually labelled subset D_o , it cannot guarantee an optimal solution for the entire dataset D . Nonetheless, OPAL uses three mechanisms to ensure that its labelling performance across D

closely approximates an optimal solution to problem (*). First, before solving problem (*), OPAL fine-tunes the underlying classifiers using a separate manually labelled subset $D_t \subset D$ – disjoint from D_o – referred to as the *fine-tuning* subset, to ensure high classification accuracy on D . Second, OPAL uses diversified random sampling to select D_t and D_o , ensuring they are representative of D . Finally, the decision variables derived from exhaustively solving problem (*) on D_o are applied to the entire dataset D . Our empirical evaluation in Section V shows that these mechanisms enable OPAL to achieve near-optimal – if not exactly optimal – solutions on the full dataset and that OPAL significantly outperforms labelling methods that do not use constrained optimization.

Novelty. The key novelty of OPAL is its accuracy-driven labelling process, which explicitly controls a target accuracy threshold while optimizing labelling effort. Further, we show that OPAL’s labelling process – corresponding to problem (*) – can be formulated as an MILP and solved efficiently. To our knowledge, our effort-optimized, accuracy-driven formulation for data labelling is novel. Although one could, in principle, solve problem (*) using alternatives such as genetic algorithms [22] or a brute-force search, these approaches have notable limitations. Heuristic methods (e.g., genetic algorithms) do not provide exhaustive search or deterministic reproducibility, whereas MILP solvers [16], [17], [23] ensure both. Brute-force approaches are also impractical due to their inability to handle floating-point decision variables and their poor scalability with increasing dimensionality – our formulation involves real-valued decision variables and the number of constraints in our formulation grows with the number of classifiers. Finally, while machine learning models can be used for optimization tasks, they cannot solve constrained optimization problems that require strict enforcement of constraints (e.g., ensuring Accuracy $\geq \alpha$). Consequently, MILP remains the preferred approach for our formulation.

Significance. A 2021 study by Northcutt et al. [14] found that many labels in the test sets of popular datasets are incorrect, for example, reporting labelling error rates of 5.8% for ImageNet [21] and 10.1% for QuickDraw [24]. The authors observed that mislabelled test sets can significantly distort model validation and verification. Notably, in their experiments, models that performed poorly on benchmarks such as ImageNet and QuickDraw turned out to be among the most accurate once the labelling errors in the benchmarks were corrected [14]. OPAL aims to improve the quality of data labelling, particularly in the context of testing, by enabling practitioners to directly control their accuracy target while minimizing labelling effort accordingly. To achieve this, OPAL identifies difficult instances that, based on the chosen accuracy target, pretrained classifiers cannot confidently label. These instances are delegated to human annotators, while the remaining data is labelled automatically.

III. BACKGROUND

A. Mixed-Integer Linear Programming (MILP)

Constrained optimization finds values for decision variables that satisfy a set of equality and inequality constraints while

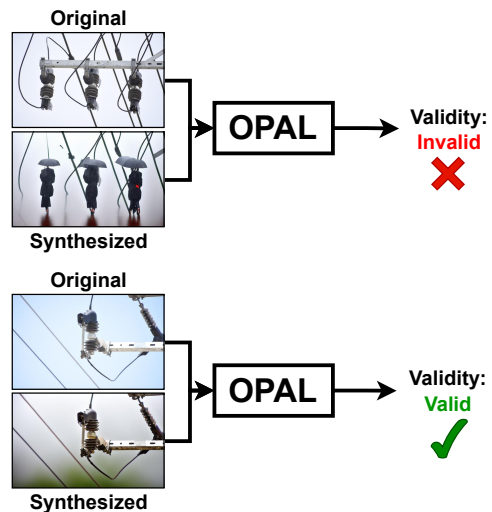


Fig. 1: Illustrating the application of OPAL for test-input validation. An image and its transformation are provided to OPAL. OPAL determines whether the transformed image is an acceptable and valid alteration of the original image.

minimizing or maximizing an objective function [16]. Linear Programming (LP) is a subclass of constrained optimization techniques in which both the objective and the constraints are linear and all variables are continuous. Mixed-Integer Linear Programming (MILP) extends LP by enforcing integrality on some variables to capture discrete decisions (e.g., selecting modules or features). In software engineering, constrained optimization techniques such as MILP and LP have been applied to reliability optimization, effort estimation, decision support, and product-line configuration, e.g., [25]–[27]. In this article, we formulate the tasks of test-input labelling and test-input validation as MILP problems, with the goal of building high-accuracy test sets while minimizing manual effort.

B. Testing Vision Systems

As motivated in Section I, we evaluate OPAL by applying it in the context of vision-system testing. Vision systems, being based primarily on deep learning and machine learning, do not have traditional specifications [2]. This leads to two important challenges in testing vision systems: (Challenge 1) Developing test oracles, i.e., test-input labels, remains largely a manual task; and (Challenge 2) Test-generation methods for such systems, e.g., metamorphic testing [3], [4], [7], [28], may produce invalid test inputs, necessitating further automated measures to determine test-input validity.

OPAL helps address both of the above challenges. With regard to the first challenge, OPAL can be employed to automatically produce labels, i.e., test oracles, for test data, providing explicit control over the trade-off between accuracy and manual effort. We refer to such a use case of OPAL as **automated test-data labelling**. With regard to the second challenge, when provided with a pair of test-data images – where one is the original image and the other is a transformed version of the original – OPAL can determine whether the pair is valid or not. Valid pairs are those in which the transformed

image is an acceptable alteration of the original image. For instance, Figure 1 shows an example where a generative AI technique (more specifically, Stable Diffusion [29]) has added a rain effect to an original image, and the task is to validate whether the transformation is a valid one. Here, OPAL identifies the top transformation in Figure 1 as an invalid test input, since in the transformation, the high-voltage fuse cutouts on the utility pole have been mistaken as humans, and the rain effect has been added by altering the cutouts and giving them umbrellas. The bottom pair is identified as valid, since the transformed image retains the content of the original image and only modifies the weather condition in the original image. We refer to this second use case of OPAL as **automated test-data validation**. As with the first use case, OPAL provides explicit control over the trade-off between accuracy and manual effort.

In this article, we systematically evaluate OPAL for both the automated test-data labelling use case (RQ1 and RQ2 in Section V) and the automated test-input validation use case (RQ3 in Section V). Our evaluation results show that OPAL is an effective tool for both use cases in the context of testing vision systems, outperforming state-of-the-art baselines.

C. Active Learning

Active learning is an iterative, human-in-the-loop approach designed to improve the accuracy of machine learning models while reducing annotation effort. In each iteration of active learning, only the most uncertain samples are sent to human annotators for labelling, while the rest are automatically labelled by the model. The model is then retrained on the expanded labelled dataset that includes the newly annotated samples [30]. This approach concentrates human effort where it most benefits accuracy, thus lowering manual effort [8], [30]. Recent work has shown that active learning can be effectively applied to test-input validation by training lightweight machine-learning models on image features [8]. Therefore, to evaluate OPAL for test-input validation, we also consider an extension with active learning to examine its potential for further reducing manual effort.

IV. OPTIMIZED LABELLING VIA MILP

Algorithm 1 details OPAL. It takes as input an unlabelled dataset D , an accuracy threshold α , a set of n pretrained classifiers, a percentage $hInitial$ of D to be manually labelled initially, and the size s of the subset $D_o \subset D$ used for optimization. Ultimately, for our evaluation, we measure the proportion of D labelled manually versus automatically. Hence, we define $hInitial$ as the fraction of D that OPAL requires to be manually labelled initially (i.e., the set $D_t \cup D_o$), and then partition this fraction into D_t and D_o so that $|D_o| = s$. We specify $|D_o|$ directly via the input parameter s , rather than as a fraction of D , because $|D_o|$ determines the number of constraints in the MILP used to solve problem (*). The output of OPAL is the labelled dataset D , with some elements manually labelled and the rest labelled by the classifiers.

Assumptions. OPAL makes two assumptions about the classifiers c_1, \dots, c_n : (1) they are pretrained, and (2) for each

Algorithm 1 Effort-Optimized Accuracy-Driven Labelling (OPAL) using mixed-integer linear programming (MILP)

Input D : An unlabelled dataset

Input α : Accuracy threshold

Input c_1, \dots, c_n : A set of pretrained classifiers

Param $hInitial$: Percentage of D for fine-tuning and decision variable computation

Param s : Number of elements used for computing decision variables using MILP

Output D : Labelled dataset

```

// Step 1. Data splitting
1: ( $D_t, D_o, D'$ ) = DataSplit( $D, hInitial, s$ ) //  $\frac{|D_t \cup D_o|}{|D|} = hInitial, |D_o| = s$ 
//  $D_t, D_o$ , and  $D'$  are for fine-tuning, optimization, and labelling, respectively.
2: Manually label  $D_t \cup D_o$ 
// Step 2: Fine tuning
3: FineTune( $(c_1, \dots, c_n), D_t$ )
// Step 3: Computing decision variables using MILP
4: ( $\omega_1, \dots, \omega_n$ ) = MILPSolver( $(c_1, \dots, c_n), D_o, \alpha$ )
// Step 4: Labelling  $D'$  using  $\omega_1, \dots, \omega_n$ 
5:  $D_m = \emptyset$  // A subset of  $D'$  to be manually labelled on Line 17
6: for  $e_i \in D'$  do
7:   for  $j \in \{1..n\}$  do
8:     Let  $\hat{l}_{ji}$  be the predicted label for  $e_i$  by  $c_j$ 
9:     Let  $\hat{\theta}_{ji}$  be the prediction confidence for  $e_i$  by  $c_j$ 
10:  end for
// Labelling decision (Condition 1 and Condition 2)
11:  if  $\hat{l}_{1i} = \dots = \hat{l}_{ni}$  and  $\omega_1 \hat{\theta}_{1i} + \dots + \omega_n \hat{\theta}_{ni} > 1$  then
12:    Label( $e_i$ ) =  $\hat{l}_{1i}$ 
13:  else
14:     $D_m = D_m \cup \{e_i\}$ 
15:  end if
16: end for
17: Manually label  $D_m$ 
18: return the labelled set  $D$ 

```

element $e \in D$, each classifier labels e with a confidence indicating how certain the classifier is about its prediction. Otherwise, there is no restriction on the type and nature of data in D .

The four steps of Algorithm 1 are discussed below:

Data Splitting (Step 1). OPAL partitions the unlabelled dataset D into three subsets: a *fine-tuning subset* D_t , an *optimization subset* D_o , and a *to-be-labelled subset* denoted by D' (Line 1). The subset D_t is used to fine-tune the pretrained classifiers in Step 2; D_o is used for optimization in Step 3; and in Step 4, each element in D' is labelled either automatically (Line 12) or manually (Line 17).

Specifically, OPAL partitions D into clusters by grouping elements with high similarity (or proximity) according to a relevant distance metric. Next, it draws an equal number of elements from each cluster until an $hInitial$ proportion of D is selected. This sampling strategy increases the diversity of

the selected samples and helps them be more representative of D . The sampled subset is then divided randomly into two sets: D_t and D_o such that $|D_o| = s$. The sets D_t and D_o are then manually labelled (Line 2).

Fine-tuning (Step 2). OPAL fine-tunes the classifiers using the subset D_t (Line 3). Since retraining from scratch is both computationally expensive and requires extensive labelled data, as mentioned earlier in our assumptions, OPAL leverages pretrained classifiers. Fine-tuning the classifiers on the subset D_t increases their accuracy for the dataset D .

Computing decision variables using MILP (Step 3). OPAL formulates the constrained optimization problem $(*)$ as an MILP problem and solves it for the set D_o (Line 4). For each $e_i \in D_o$, each classifier c_j generates a label \hat{l}_{ji} with confidence $\hat{\theta}_{ji}$. We introduce decision variables $\omega_1, \dots, \omega_n$ corresponding to classifiers c_1, \dots, c_n . Each variable ω_j is a weight signifying how much credibility should be given to classifier c_j for labelling. OPAL automatically labels an element e_i when these two conditions hold:

(Condition 1) $\hat{l}_{1i} = \dots = \hat{l}_{ni}$ (i.e., all classifiers label e_i the same)

(Condition 2) The weighted sum $\omega_1 \hat{\theta}_{1i} + \dots + \omega_n \hat{\theta}_{ni}$ is higher than a threshold

Without loss of generality, we assume the threshold is 1 (one), as any other value would allow us to normalize all the weights, $\omega_1, \dots, \omega_n$, by dividing them by that value. Specifically, we write Condition 2 as follows: $\omega_1 \hat{\theta}_{1i} + \dots + \omega_n \hat{\theta}_{ni} \geq 1$.

For each $e_i \in D_o$, we define the predicate z_i and the variable x_i to represent Condition 1 and Condition 2 for e_i , respectively:

$$z_i = \begin{cases} 1; & \hat{l}_{1,i} = \dots = \hat{l}_{n,i} \\ 0; & \text{Otherwise} \end{cases}, \quad x_i = \begin{cases} 1; & \omega_1 \hat{\theta}_{1i} + \dots + \omega_n \hat{\theta}_{ni} > 1 \\ 0; & \text{Otherwise} \end{cases} \quad (1)$$

Predicates z_i have known values. However, variables x_i depend on the weights ω_j that need to be determined via optimization. Hence, similarly to the weights ω_j , the variables x_i are also considered decision variables in our formulation.

We formalize the Manual Effort in problem $(*)$ as the number of elements that would be assigned to the human labeller, noting that OPAL automatically labels e_i if Conditions 1 and 2 hold – i.e., both x_i and z_i are one. Otherwise, e_i is assigned to a human labeller if $x_i z_i = 0$.

$$\text{Manual Effort} = |\{e_i \in D_o \mid z_i x_i = 0\}| = \sum_{i=1}^{|D_o|} (1 - z_i x_i) \quad (2)$$

We now formalize Accuracy in problem $(*)$. Accuracy is defined as the proportion of elements in D_o that are labelled correctly by OPAL, whether automatically or manually. Only those elements labelled automatically by OPAL can potentially be labelled incorrectly. We define the intermediary predicates b_i to indicate whether all classifiers label e_i correctly according to its ground-truth label:

$$b_i = \begin{cases} 1; & l_i = \hat{l}_{1,i} = \dots = \hat{l}_{n,i} \\ 0; & \text{Otherwise} \end{cases}$$

where l_i is the ground-truth label of e_i . OPAL labels an element e_i incorrectly (and hence automatically) if $x_i z_i = 1$

and $x_i b_i = 0$. Stated otherwise, OPAL correctly labels e_i if $x_i z_i = 0$ or $x_i b_i = 1$. Given this, we formalize accuracy as the complement of the proportion of elements in D_o that are incorrectly (and automatically) labelled.

$$\text{Accuracy} = 1 - \frac{\sum_{i=1}^{|D_o|} (z_i x_i - b_i x_i)}{|D_o|} = \frac{|D_o| + \sum_{i=1}^{|D_o|} (b_i - z_i) x_i}{|D_o|}$$

We now rewrite the constraint $\text{Accuracy} \geq \alpha$ as follows:

$$\frac{|D_o| + \sum_{i=1}^{|D_o|} (b_i - z_i) x_i}{|D_o|} \geq \alpha \implies \sum_{i=1}^{|D_o|} (b_i - z_i) x_i + |D_o|(1 - \alpha) \geq 0 \quad (3)$$

Equation 1 relates variables x_i to weights ω_j through a case-based function which is non-linear. Following the standard practice in linear programming [16], [17], we linearize this relationship by introducing the following two constraints:

$$\begin{aligned} \omega_1 \hat{\theta}_{1i} + \dots + \omega_n \hat{\theta}_{ni} - 1 &\leq M x_i \\ \omega_1 \hat{\theta}_{1i} + \dots + \omega_n \hat{\theta}_{ni} - 1 &\geq -M(1 - x_i) + \epsilon \end{aligned}$$

where M is a large constant, e.g., 10^6 , and ϵ is a small positive value, e.g., 10^{-6} . These constraints force each variable x_i to be either one when $\omega_1 \hat{\theta}_{1i} + \dots + \omega_n \hat{\theta}_{ni} > 1$, or zero when $\omega_1 \hat{\theta}_{1i} + \dots + \omega_n \hat{\theta}_{ni} \leq 1$. Note that when $\omega_1 \hat{\theta}_{1i} + \dots + \omega_n \hat{\theta}_{ni} = 1$, the presence of ϵ in the second inequity ensures that x_i is 0.

Using Equation (2), Constraint (3) and the above two constraints, we obtain the following characterization of our constrained optimization problem $(*)$:

$$\begin{aligned} &\text{minimize}_{\omega_1, \dots, \omega_n, x_1, \dots, x_{|D_o|}} |D_o| - \sum_{i=1}^{|D_o|} z_i x_i \\ &\text{subject to} \quad \sum_{i=1}^{|D_o|} (b_i - z_i) x_i + |D_o|(1 - \alpha) \geq 0 \quad \wedge \\ &\quad \bigwedge_{i=1, \dots, |D_o|} \omega_1 \hat{\theta}_{1i} + \dots + \omega_n \hat{\theta}_{ni} - 1 \leq M x_i \quad \wedge \\ &\quad \bigwedge_{i=1, \dots, |D_o|} \omega_1 \hat{\theta}_{1i} + \dots + \omega_n \hat{\theta}_{ni} - 1 \geq -M(1 - x_i) + \epsilon \end{aligned}$$

The minimization objective and the constraints in the above are all linear with respect to the floating-point decision variables $\omega_1, \dots, \omega_n$, and the binary decision variables $x_1, \dots, x_{|D_o|}$. Hence, the above optimization problem is an MILP problem and can be solved using MILP solvers [16], [17], [23]. Our MILP formulation includes $n + |D_o|$ decision variables and $2|D_o| + 1$ constraints. As demonstrated in Section VI, the MILP solver takes significantly less than the other three steps while enabling OPAL to achieve a very high level of accuracy.

Labelling (Step 4). OPAL labels D' , i.e., the remaining unlabelled subset of D , using the $\omega_1, \dots, \omega_n$ values obtained from solving the constrained optimization problem in Step 3. First, each classifier generates a label and a confidence score for each element in D' (Lines 7–10). Then, if both Conditions 1 and 2 hold, elements are automatically labelled. Otherwise, elements are stored in a set D_m to be manually labelled at the end (Line 17). Once all the elements are labelled, OPAL returns the labelled set D (Line 18).

V. EVALUATION SETUP

We evaluate OPAL on seven image datasets: five containing real-world images and three containing synthetic images specifically generated for testing vision-based systems. Our evaluation aims to answer the three research questions (RQs) described below. As discussed in Section III-B, OPAL can be used in two distinct scenarios for improving the testing of DL systems: (1) using OPAL for test-data labeling, and (2) using OPAL for test-input validation. RQ1 and RQ2 evaluate OPAL for test-data labeling and compare it against test-data labeling baselines, whereas RQ3 evaluate OPAL for test-input validation and compare it against test-input validation baselines.

RQ1. (OPAL’s test-data labelling effort and accuracy)

How close does OPAL come to perfect accuracy, and how much manual labelling is required to achieve peak (near-perfect) accuracy? We configure OPAL by setting α in Algorithm 1 to 100% to push OPAL to reach its upper bound in terms of accuracy. We then evaluate OPAL by systematically varying the algorithm’s inputs, including the set of input classifiers and the parameter $hInitial$, which represents the amount of manually labelled data used for fine-tuning and optimization.

We measure both the labelling accuracy and the total labelling effort. Note that the parameter $hInitial$ determines the initial labelled set for fine-tuning and optimization, while the total effort additionally includes the set D_m , which is manually labelled at the end of Algorithm 1. Based on these results, we provide insights into how many classifiers and how much pre-labelled data ($hInitial$) would be required for OPAL to achieve near-perfect accuracy with minimal overall labelling effort.

RQ2. (Comparison with state-of-the-art test-data labelling baselines) *Given the same manual labelling effort used by OPAL in RQ1 to achieve near-perfect accuracy, can state-of-the-art methods achieve a comparable level of labelling accuracy?* RQ2 compares OPAL with state-of-the-art supervised and semi-supervised methods for image labelling. We provide the baselines with the same amount of manually labelled elements that OPAL needs for reaching near-perfect accuracy in RQ1. We then compare their labelling accuracy to OPAL’s.

RQ3. (OPAL for test-input validation) *How does OPAL compare to state-of-the-art baselines for test-input validation?* In this research question, we evaluate OPAL for test-input validation in two ways. First, we apply OPAL as described in Algorithm 1 for validating test-inputs. Second, we extend OPAL with an active-learning loop, as detailed in Section III-C, and then apply it for test-input validation. We compare OPAL, both with and without active learning, against state-of-the-art baselines [3], [4], [8].

A. Baselines

We compare OPAL with two groups of baselines: baselines for test-data labelling and baselines for test-input validation. Both groups of baselines are detailed and described below.

Algorithm 2 Image Labelling via Supervised Learning [18]–[20]

Input D : An unlabelled dataset

Input c : A pretrained classifier

Param $hTotal$: Percentage of D to be manually labelled for supervised learning

Output D : Labelled dataset

```

// Step 1: Data splitting
1:  $(D_t, D')$  = DataSplit( $D, hTotal$ ) //  $D = D_t \cup D'$ ,  $\frac{|D_t|}{|D|} = hTotal$ 
2: Manually label  $D_t$ 
// Step 2: Fine tuning
3: FineTune( $c, D_t$ )
// Step 3: Labelling  $D'$ 
4: for  $e_i \in D'$  do
5:   Let  $\hat{l}_i$  be the predicted label for  $e_i$  by  $c$ 
6:   Label( $e_i$ ) =  $\hat{l}_i$ 
7: end for
8: return the labelled set  $D$ 

```

1) *Test-data labelling baselines:* We consider techniques for building highly accurate classifiers, noting that, once trained, these classifiers can automatically label unlabelled datasets. In particular, we consider (1) *supervised learning* [18]–[20], the standard approach for training classifiers, and (2) *pseudo-labelling* [9], [11], a state-of-the-art semi-supervised learning technique that offers an effective strategy for achieving high classification accuracy when most of the training data is unlabelled and only a small portion is labelled. Empirical studies indicate that pseudo-labelling is an effective method across various domains and consistently outperforms established baselines [9], [11], [31]. Below, we outline the approaches underlying supervised learning and pseudo-labelling. The specific instantiations used in our evaluation are described in Section VI.

Supervised Learning Baseline. Algorithm 2 outlines labelling via supervised learning. The algorithm takes as input an unlabelled dataset D , the percentage $hTotal$ of D for manual labelling and a classifier c , and labels D in three steps. First, D is split into two subsets: a *fine-tuning* subset D_t and a *to-be-labelled* subset D' where D_t comprises a fraction $hTotal$ of D (Line 1 in Algorithm 2). Then, the fine-tuning subset D_t is manually labelled (Line 2 in Algorithm 2). Second, the classifier is fine-tuned on D_t (Lines 3 in Algorithm 2). Third, the fine-tuned classifier labels all the elements in D' and the labelled set $D_t \cup D'$ is returned.

Pseudo-labelling Baseline. Algorithm 3 presents the pseudo-labelling approach, as introduced by Lee et al. [11] and Pham et al. [9]. The algorithm receives as input an unlabelled dataset D , the percentage $hTotal$ of D for manual labelling, the size v of the validation set, and a classifier c . It labels D in two steps. First, D is divided into three subsets: a *fine-tuning* subset D_t , a *validation* subset D_v , and a *to-be-labelled* subset D' . The fine-tuning and validation subsets together constitute a proportion $hTotal$ of the input dataset. From this portion, v elements are randomly selected to form the validation set D_v , while the remainder is used as the fine-tuning set D_t (Line 1 in Algorithm 3). The fine-tuning subset D_t and the validation subset D_v are manually labelled (Line 2 in Algorithm 3). Second, the algorithm iteratively generates pseudo-labels –

Algorithm 3 Image Labelling via Pseudo Labelling [9], [11]

Input D : An unlabelled dataset
Input c : A pretrained classifier
Param $hTotal$: Percentage of D to be manually labelled for semi-supervised learning
Param v : Number of elements used for validation
Output D : Labelled dataset

```

// Step 1: Data splitting
1:  $(D_t, D_v, D') = \text{DataSplit}(D, hTotal, v) // \frac{|D_t \cup D_v|}{|D|} = hTotal, |D_v| = v$ 
2: Manually label  $D_t$  and  $D_v$ 
// Step 2: Iterative pseudo-labelling
3: while  $\neg$  OverFitted( $c, D_t, D_v$ ) and time budget is not over do
// Generate pseudo labels for  $D'$ 
4:   for  $e_i \in D'$  do
5:     Let  $\hat{l}_i$  be the predicted label for  $e_i$  by  $c$ 
6:     Label( $e_i$ ) =  $\hat{l}_i$ 
7:   end for
// Fine-tune  $c$  using ground-truth-labelled and pseudo-labelled data
8:   FineTune( $c, D_t \cup D'$ )
9: end while
10: return the labelled set  $D$ 

```

labels produced by the classifier itself – for the unlabelled subset D' . It then fine-tunes the classifier on the combined dataset $D_t \cup D'$, which includes both ground-truth and pseudo-labelled data (Lines 4–9 in Algorithm 3). The loop ends either when the classifier begins to overfit or when the time budget is reached. Specifically, Algorithm 3 uses the validation set D_v to detect overfitting: if c 's accuracy on D_t is significantly higher than c 's accuracy on D_v , it signals overfitting.

Compared to Algorithm 2, Algorithm 3 offers a key advantage by treating pseudo-labels as ground truth for training c . In this way, the absence of ground-truth labels for some data elements does not prevent the classifier from learning from them. Hence, the classifier is trained on a larger, more diverse set of examples.

2) *Test-input validation baselines*: We consider state-of-the-art techniques from the literature [3], [4], [8]. Each baseline receives a pair of images – one original and one transformed – and determines the validity of the transformation using image-comparison metrics [32]. These metrics quantify how closely a transformed image aligns with its corresponding original. Below, we outline these baselines which we refer to as *B-VIF* [3], *B-VAE* [4], *B-HiL-TV1* [8], and *B-HiL-TV2* [8]:

B-VIF Baseline [3]: The B-VIF baseline computes the Visual Information Fidelity (VIF) metric [33] to compare each transformed image against its original. Given a dataset, B-VIF uses a manually pre-validated subset to select an optimized threshold for the VIF values to distinguish between valid and invalid pairs. It then uses the threshold to automatically validate the remaining images in the dataset. The manual effort of this baseline is then the size of the manually pre-validated subset, and its accuracy is measured by how well it classifies the remaining data automatically.

B-VAE Baseline [4]: The B-VAE baseline uses the variational autoencoder (VAE) reconstruction-error approach of Riccio and Tonella [4] as its image-comparison metric. To compute this metric, a VAE is trained on the original images in a given dataset to learn their distribution. Provided with a trained VAE, B-VAE automatically validates each transformed

image by computing its reconstruction error and comparing the error against an optimized threshold. As with the B-VIF baseline, this method uses a manually pre-validated subset of images to determine the optimized threshold that separates valid from invalid pairs. The manual effort therefore equals the size of this pre-validated subset, and the baseline's accuracy is evaluated by how well it automatically classifies the remaining data.

B-HiL-TV1 Baseline [8]: The B-HiL-TV1 baseline uses 13 image-comparison metrics, including VIF and VAE reconstruction error – used respectively by the B-VIF and B-VAE baselines already described – to validate transformed images. Unlike B-VIF and B-VAE, which use a single metric, B-HiL-TV1 trains a random-forest classifier on all the 13 computed metrics to classify transformed images as valid or invalid. Specifically, it uses a manually pre-validated subset of images to train the random-forest classifier. The classifier is then applied to the remaining data. The manual effort is determined by the size of the pre-validated subset, and the baseline's accuracy is evaluated based on how well it classifies the remaining data.

B-HiL-TV2 Baseline [8]: The B-HiL-TV2 baseline extends B-HiL-TV1 with an active-learning loop. Like B-HiL-TV1, B-HiL-TV2 uses a manually pre-validated dataset to train a random-forest classifier. Within the active-learning loop, the random-forest classifier labels transformed images as valid or invalid. Based on a confidence threshold for the predictions, only high-confidence predictions are accepted. A small number of images with low-confidence predictions are selected for manual validation. B-HiL-TV2 then re-trains the random-forest classifier by adding the newly labelled images to the existing training set and repeats the active-learning loop until all transformed images are validated. The manual effort for this baseline includes both the pre-validated subset and the images selected for manual validation in each iteration of active learning. B-HiL-TV2 has two user-specified parameters: (1) the confidence threshold used to determine when predictions from the random-forest classifier are accepted, and (2) the maximum number of images sent for manual validation in each iteration of active learning.

B. Datasets

Table I summarizes the properties of the seven datasets used in our evaluation. CIFAR-10 [34], FASHIONMNIST [35], MNIST [36], and SVHN [37] are widely used benchmarks containing real-world images. SYNTHETIC-PUB1 and SYNTHETIC-PUB2 [3] are public datasets with synthetically generated images, while INDUSTRY is a proprietary industrial dataset also consisting of synthetic images.

Below, we outline the key characteristics of our datasets, along with how we obtain ground-truth labels for those that were not pre-labelled. In our experiments, we simulate manual labelling by using ground-truth labels. As such, for the purpose of evaluation, ground-truth labels are required for the entire datasets used in our experiments, though outside this context, OPAL only needs a subset of images to be manually labelled—specifically, the $D_t \cup D_o$ set and the D_m set requested for labelling on Line 17 of Algorithm 1.

TABLE I: Properties of the datasets used in our evaluation

Dataset	Dataset Size	Public / Proprietary	Real-World / Synthetic	No of Classes
CIFAR10 [34]	70,000	Public	Real-World	10
FASHIONMNIST [35]	70,000	Public	Real-World	10
MNIST [36]	70,000	Public	Real-World	10
SVHN [37]	73,257	Public	Real-World	10
SYNTHETIC-PUB1 [3]	2,318	Public	Synthetic	2
SYNTHETIC-PUB2 [3]	5,204	Public	Synthetic	2
INDUSTRY [8]	3,000	Proprietary	Synthetic	2

* The public datasets highlighted with are pre-labelled; the synthetic, public datasets highlighted with are labelled via crowd-sourcing (Section V-B); and the synthetic, industry dataset highlighted with is labelled by third-party manual labellers and the labels are reviewed by industry experts (Section V-B)

CIFAR-10 [34] contains 32×32 coloured real-world images in 10 different classes, each class comprising 6,000 images, totalling 60,000 images. The classes include common objects such as automobile, airplane, bird, etc.

FASHION MNIST [35] contains 28×28 grayscale real-world images of fashion items in 10 classes, with each class comprising 6,000 images, totaling 60,000 images. The classes include clothing and accessories such as t-shirt, dress, sneaker, etc.

MNIST [36] contains 28×28 grayscale images of hand-written digits in 10 classes, with each class comprising approximately 6,000 training and 1,000 test images, totaling 60,000 images. The digits range from 0 to 9, commonly used for digit recognition tasks.

SVHN [37] contains 32×32 colour images of house numbers in 10 classes, each class comprising varying numbers of samples, totalling over 600,000 images. The dataset consists of real-world house-number images obtained from Google Street View.

SYNTHETIC-PUB1 and SYNTHETIC-PUB2 are obtained from the public datasets developed by Hu et al. [3]. Their objective was to create synthetic images for testing vision-based systems. To achieve this, they applied four safety-related image transformations – *brightness*, *frost*, *contrast*, and *JPEG compression* – using the Albumentations library [38] on images from the CIFAR-10 [34] and ImageNet [21] datasets. Specifically, from both CIFAR-10 and ImageNet, they selected the car-class images and an equal number of images from other classes (e.g., cat and ship classes), treating them as the not-car class. The transformed images may either preserve their essential content, remaining recognizable by humans as having the same label as their corresponding original images, or they may lose their meaning entirely. To determine the labels of the transformed images, Hu et al. presented each transformed image to five human labellers, who were asked to label each transformed image as “car” or “not car”. We performed a quality review of the images in Hu et al.’s datasets and removed images with multiple inconsistent labels from human labellers when the inconsistencies could not be resolved by majority voting. In the end, we obtained 1,574 unique labelled, synthesized images in SYNTHETIC-PUB1 based on the transformed images from CIFAR-10 and 4,034 unique

labelled, synthesized images in SYNTHETIC-PUB2 based on the transformed images from ImageNet.

INDUSTRY is a proprietary dataset developed in collaboration with an industry partner. This dataset contains synthetic images generated for robustness testing of vision-based anomaly detection solutions for identifying faults in electric transmission lines. The dataset includes images synthesized from real-world pictures of utility poles using a prompt-based generative transformer to depict different climatic conditions that were not represented in the original, real-world images. To label the transformed images, two independent labellers, who are not a co-author of this article, were trained using detailed guidelines provided by our partner. They were then asked to label the images as either “valid” or “invalid”, where “valid” indicates that the image clearly depicts a utility pole, while “invalid” means the image either does not represent a utility pole or is too distorted to be reliably identified as one. After removing the images where the labellers disagreed on the classification, 3,000 labelled images were reviewed and verified by experts from our industry partner and included in our INDUSTRY dataset.

We use all seven datasets to evaluate OPAL for test-data labelling. For test-input validation, three datasets – SYNTHETIC-PUB1, SYNTHETIC-PUB2, and INDUSTRY – are applicable, as they contain image pairs. The remaining four datasets do not include image pairs and are therefore not applicable to the test-data validation use case.

C. Evaluation Metrics

We evaluate OPAL and our baselines using three metrics. The first metric is **accuracy**, defined as the percentage of correctly labelled images in an entire dataset. Specifically, for Algorithms 1, 2, and 3, accuracy is calculated as the percentage of images correctly labelled – either automatically or manually – in dataset D .

The second metric is **manual labelling effort**, defined as the ratio of the number of manually labelled images to the size of the entire dataset. As discussed in Section V-B, since ground-truth labels are available for all of our experimental datasets, we simulate human labelling by using the corresponding labels for each image from the ground truth. This approach, commonly used in the evaluation of image classifiers [8], [39], eliminates the need for direct human input. For OPAL, the manual labelling effort is the sum of the percentage of initially labelled images, $hInitial$, and the size of set D_m , which is manually labelled on Line 17 of Algorithm 1, divided by the size of D . For the baselines presented in Algorithms 2 and 3, the manual labelling effort is simply the percentage of labelled images, $hTotal$, which is an input to these algorithms.

The last metric is the **execution time** of each labelling technique. Although neither OPAL nor the baselines rely on user feedback during their main labelling loop – since manual labelling occurs either before or after automated labelling – execution time still has practical implications. Execution time is particularly important when engineers need to label large datasets or frequently update labels in response to data changes. Therefore, we consider execution time to assess and compare the efficiency of OPAL and the baselines.

TABLE II: Classifiers used as inputs to Algorithms 1, 2, and 3

Classifier	Description
VGG [18]	Convolutional Neural Network - 16 Layers
ResNet [19]	Convolutional Neural Network with Residual Connections - 50 Layers
ViT [20]	Transformer-Based Neural Network - 12 Blocks

D. Implementation

The experiments were conducted on a machine with two Intel Xeon Gold 6338 CPUs, 512 GB of RAM, and one NVIDIA A40 GPU (46 GB memory). We have implemented OPAL in Python 3.11 using Pytorch [40] for classifiers, PuLP [23] for MILP solver and Scikit-learn [41] for data splitting and clustering.

VI. EXPERIMENTS AND RESULTS

In this section, we present the experiments performed based on the setup described in Section V to answer RQ1 and RQ2.

RQ1 experiments. To address RQ1, we run Algorithm 1 with $\alpha = 100\%$ for each of the seven datasets in Table I. Configuring OPAL requires selecting which classifiers (and how many) to include, as well as setting the parameters $hInitial$ and s .

For the choice of classifiers, we use the three state-of-the-art vision-based models listed in Table II: VGG (a CNN), ResNet (a CNN with residual connections), and ViT (a transformer-based model). These classifiers represent the main deep-learning architectures for vision-based systems. We run OPAL using different combinations of these classifiers, specifically with one, two, and all three models from Table II. We denote these configurations as $OPAL(n = 1)$, $OPAL(n = 2)$, and $OPAL(n = 3)$, respectively. In $OPAL(n = 1)$, each of the three models is used individually, producing three separate instances. In $OPAL(n = 2)$, we form three pairs (VGG+ResNet, VGG+ViT, and ResNet+ViT). Finally, $OPAL(n = 3)$ uses all the three models together (VGG+ResNet+ViT).

We vary the $hInitial$ parameter, i.e., the portion of initially labelled data, setting it to 1%, 5%, 15%, 25%, 35%, and 45% of the entire input dataset D . We set s , i.e., the size of D_o , to either 1000 or half of $hInitial$ multiplied by the size of D , whichever is smaller. This ensures that the number of constraints in OPAL’s MILP formulation remains around 2000. With this value of $|D_o|$, the MILP’s objective function – i.e., human effort – starts to saturate, and increasing $|D_o|$ further does not yield additional improvements in minimizing human effort for the set D_o . To mitigate randomness, we repeat each experiment five times. Overall, for RQ1, we perform $7(Datasets) \times 7(DL-model\ Combinations) \times 6(hInitial) \times 5(Repetitions) = 1470$ experiments.

For the data splitting step of OPAL, we first represent images in D as latent-space vectors obtained from the pretrained VGG model [18]. These vectors are then clustered using the DBSCAN algorithm [42]. The algorithm’s parameters, namely, epsilon and the minimum number of samples per cluster, are configured in accordance with established best practices [42], [43]. The fine-tuning step of OPAL uses 20 epochs with batch sizes and learning rates set according to

TABLE III: Average percentage of images satisfying Condition 1 and Condition 2, both individually and together, in Algorithm 1 as the number of classifiers (n) increases

Conditions being fulfilled	n=1	n=2	n=3
Condition 1	All	65.2%	62.7%
Condition 2	34.4%	44.0%	58.9%
Condition 1 and Condition 2	34.4%	41.6%	51.7%

the recommended configurations for each classifier. The code and data are available [44].

RQ1 results. Figure 2 shows a scatter plot of accuracy versus manual labelling effort, where each point corresponds to an experiment performed for a specific dataset, a particular value of $hInitial$, and one of the three configurations $OPAL(n = 1)$, $OPAL(n = 2)$, or $OPAL(n = 3)$. We use colours to differentiate between different configurations and shapes to differentiate between different datasets. With a single classifier ($n = 1$), OPAL achieves an average accuracy of 97.7% while requiring an average manual effort of 65.6%. Increasing to two classifiers ($n = 2$) boosts the average accuracy to 98.1% and reduces the average manual effort to 58.4%. Finally, using three classifiers ($n = 3$) yields the highest average accuracy of 98.4%, while further lowering the average manual effort to 48.3%. The results indicate that increasing the number of classifiers improves accuracy and substantially reduces the labelling effort. To further investigate the impact of increasing the number of classifiers on OPAL’s performance, Table III shows the average percentage of images that satisfy **Condition 1** and **Condition 2**, both individually and in conjunction, for different number of classifiers. Note that for $OPAL(n = 1)$, **Condition 1** holds vacuously for all images. As the table shows, **Condition 2** is more restrictive than **Condition 1** and is satisfied by fewer images than **Condition 1** in all cases. Given that the rates at which images satisfy **Condition 2** and the conjunction of these two conditions are close, **Condition 2** largely determines whether, or not, an image is labelled automatically. Increasing the number of classifiers makes **Condition 2** weaker and easier to satisfy, leading OPAL to automatically label more images and thereby reducing the amount of manual labelling.

While $OPAL(n = 3)$ surpasses $OPAL(n = 1)$ and $OPAL(n = 2)$ in both accuracy and manual effort, it only modestly increases execution time. Specifically, the average execution times for $n = 1$, $n = 2$, and $n = 3$ are 525, 730, and 913 seconds, respectively. Given $OPAL(n = 3)$ ’s better performance, we focus on this configuration in the rest of RQ1 and in RQ2, and in the remainder of Section VI, OPAL refers to $OPAL(n=3)$.

To examine the probability that $OPAL(n = 3)$ achieves a labelling accuracy above a given threshold, we present the complementary cumulative distribution function (i.e., $1 - CDF$) in Figure 3 computed based on the accuracy results for $OPAL(n = 3)$ from Figure 2. The three points highlighted in Figure 3 summarize the accuracy performance of $OPAL(n = 3)$ as follows: **(A)** In 99.5% of the experiments, OPAL achieves at least 89.5% accuracy. **(B)** In 95.2% of the experiments,

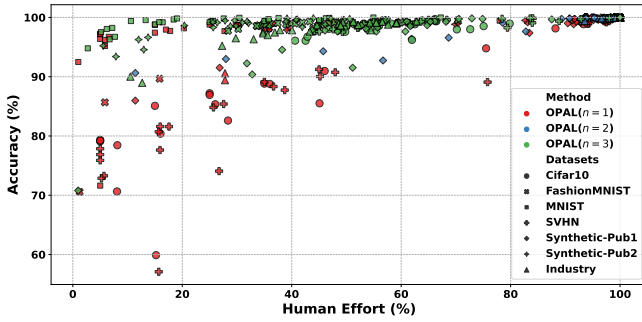


Fig. 2: Labelling accuracy vs. manual labelling effort for different configurations of OPAL, different portions of manually pre-labelled data ($hInitial$) and different datasets

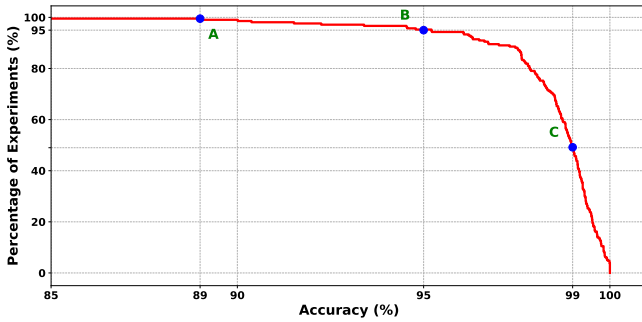


Fig. 3: The proportion of OPAL's experiments with $n=3$ from Figure 2 that achieve an accuracy at or above a specified threshold: Point (A) shows 99.5% of the experiments achieve at least 89.5% accuracy; point (B) shows 95.2% of the experiments achieve at least 95% accuracy; and point (C) shows 49.2% of the experiments achieve at least 99% accuracy

OPAL achieves at least 95% accuracy. (C) In 49.2% of the experiments, OPAL achieves a minimum accuracy of 99%.

We next explore how to configure the parameter $hInitial$. We use decision-tree analysis to identify $hInitial$ values that achieve at least 98% accuracy while keeping manual effort below 50%. These thresholds represent practical trade-offs in real-world applications. To build a decision tree that generalizes effectively across multiple datasets, we aggregate the OPAL($n = 3$) results from all seven datasets in Table I. We then split the combined dataset into two groups: data points with accuracy $\geq 98\%$ and manual effort $\leq 50\%$ are considered “desired”, while all other data points are deemed “undesired”. Figure 4 shows the resulting decision tree. At each node, the tree identifies the most influential value of $hInitial$ for classifying data points as desired or undesired. As the tree shows, the $hInitial$ values of 15%, 25% and 35% are more likely to yield the desired trade-offs than the values lower than 15% and higher than 35%. For these $hInitial$ values, OPAL($n = 3$) achieves an average accuracy of 98.8% while requiring only 44.4% manual effort.

We engaged an independent labeller – who is not an author of this study – to qualitatively analyze the images mislabelled by OPAL. We collected all mislabelled images from a single run in which OPAL was applied using three classifiers with

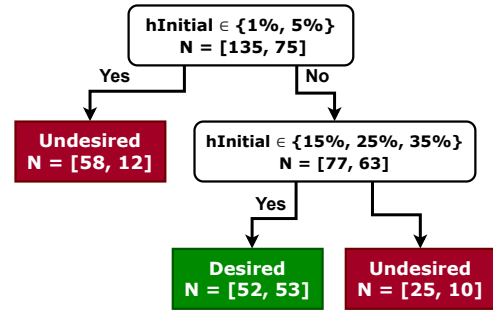


Fig. 4: Decision tree for manual pre-labelling budget ($hInitial$) in OPAL: The decision tree identifies $hInitial$ values that yield our desired performance, achieving at least 98% accuracy while keeping manual effort below 50%. At each node, $N = [x, y]$ indicates the count of undesired (x) and desired (y) experiments reaching that point

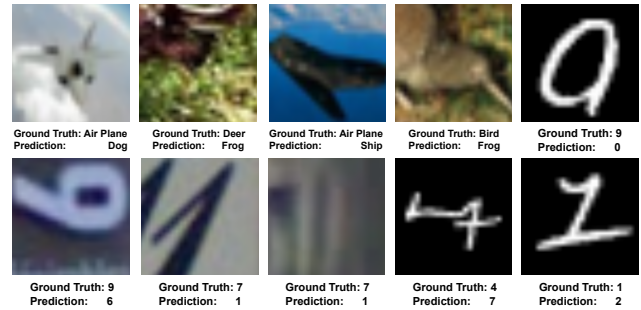


Fig. 5: Examples of images from MNIST, SVHN, SYNTHETIC-PUB1, and SYNTHETIC-PUB2 that were mislabelled by both OPAL and the human labeller, along with their ground-truth labels and the predictions made by OPAL

$hInitial = 15\%$ across our seven datasets. This resulted in a set of 1,936 images – constituting 0.6% (six-tenths of a percent) of all images in our datasets – being mislabelled by OPAL. We provided the labeller with the descriptions of our public datasets (see Section V-B) so that they knew the class labels for each dataset and requested that they label the images mislabelled by OPAL. The labeller was not aware of OPAL's labels for these images. Out of the 1,936 images, the human labeller also misclassified 561 images – about 29% – according to the ground truth. These images are available in our replication package [44]. Figure 5 shows some examples of images from MNIST, SVHN, SYNTHETIC-PUB1, and SYNTHETIC-PUB2 that were mislabelled by both OPAL and the human labeller, along with their ground-truth labels and the predictions made by OPAL. Although these problematic images make up well under 1% of the total, this finding suggests that perfect labelling accuracy may be unattainable even for human annotators due to low data quality in some datasets and the inherent subjectivity of labelling complex or low-quality images.

Finding: Based on experiments across seven diverse datasets, when OPAL is configured to target 100% accuracy, it achieves an average accuracy of 98.8%, just 1.2% below perfect accuracy, while requiring 44.4% manual effort, effectively cutting manual labelling by more than half.

Takeaway 1: When applying OPAL to vision-based classification tasks, we recommend combining multiple vision-based classifiers with different architectures – such as CNNs and transformers. Our results – consistently observed across seven datasets – show that using three distinct CNN-based and transformer-based models significantly improves accuracy and reduces manual effort compared to relying on just one or two.

Takeaway 2: Using only 1–5% of pre-labelled data for fine-tuning and optimization in OPAL yields low accuracy. Conversely, using 45% of pre-labelled data pushes manual effort above 50%, while accuracy improves only marginally. The best trade-off between accuracy and manual effort is achieved when 15–35% of the data are pre-labelled (i.e., when $h_{Initial}$ is set to 15–35%).

Takeaway 3: Among images misclassified by OPAL, approximately 30% were also misclassified by a human annotator, indicating that perfect labelling accuracy may be unattainable even for human labellers.

RQ2 experiments. To compare OPAL with baselines, i.e., Algorithms 2 and 3, we apply the baselines to the datasets in Table I and compare their results with OPAL’s results from RQ1. Configuring Algorithms 2 and 3 requires selecting a classifier and setting the parameter h_{Total} . Algorithm 3 further requires setting parameter v , i.e., the size of the validation set.

We apply the supervised learning method, i.e., Algorithm 2, to each classifier in Table II, referring to the resulting baselines as $B-VGG$, $B-ResNet$, and $B-ViT$. For the pseudo-labelling method, we execute Algorithm 3 exclusively with the VGG model since, in our preliminary experiments, VGG demonstrates the best performance among the three. Note that the pseudo-labelling baseline is substantially more expensive than supervised learning, as Algorithm 3 fine-tunes the classifier multiple times in a loop over the entire dataset. Hence, we only evaluate the pseudo-labelling baseline with VGG, referring to it as $B-Pseudo$.

The parameter h_{Total} in Algorithms 2 and 3 specifies the total amount of manual labelling effort required for supervised learning and pseudo-labelling, respectively. To ensure a fair comparison between OPAL and the baselines, i.e., that all methods operate under the same total manual labelling effort, we first calculate the average manual effort OPAL requires for each dataset in Table I, using the results from RQ1. This process yields six average manual effort values for each dataset, each corresponding to one of the six different levels of pre-labelled data – that is, the six different values for $h_{Initial}$, considered in RQ1 experiments. For each dataset, we set the parameter h_{Total} in Algorithms 2 and 3 to these six values, respectively. This ensures that OPAL and the baselines are

TABLE IV: Vargha-Delaney \hat{A}_{12} statistical test between OPAL’s labelling accuracy versus baselines. In all comparisons, we have $p\text{-value} \ll 0.01$

Dataset	With B-Pseudo	With B-VGG	With B-ResNet	With B-ViT
Cifar10	1.00 (L)	0.99 (L)	1.00 (L)	0.96 (L)
Fashion MNIST	1.00 (L)	1.00 (L)	1.00 (L)	1.00 (L)
MNIST	0.82 (L)	0.74 (L)	0.83 (L)	0.85 (L)
SVHN	0.98 (L)	0.98 (L)	0.95 (L)	0.98 (L)
Synthetic-Pub1	0.87 (L)	0.91 (L)	0.98 (L)	0.92 (L)
Synthetic-Pub2	0.86 (L)	0.86 (L)	0.97 (L)	0.84 (L)
Industry	0.93 (L)	0.93 (L)	0.97 (L)	0.91 (L)

evaluated under an identical total manual labelling budget. We set v in Algorithm 3 to 15% of the manually labelled elements, allocating the remaining 85% for fine-tuning – a common validation/fine-tuning split in the DL community [45]. To maintain consistency, we implement the data splitting and fine-tuning steps in both Algorithms 2 and 3 identically to OPAL. To address randomness, as in RQ1, we repeat each experiment five times. In total, for RQ2, we perform $4(\text{baselines}) \times 6(\text{labelling budgets}) \times 7(\text{datasets}) = 168$ experiments.

RQ2 results. Figure 6 shows the labelling accuracy of OPAL compared to the four baselines – $B-VGG$, $B-ResNet$, $B-ViT$, and $B-Pseudo$ – under the same manual labelling budget. The Wilcoxon Signed-Rank test [46] confirms that OPAL’s accuracy significantly outperforms that of all baselines ($p\text{-value} \ll 0.01$) across all datasets. Table IV presents the results of the Vargha-Delaney \hat{A}_{12} effect size test [47], comparing the accuracy of OPAL against each baseline across all datasets. According to the Vargha and Delaney classification of effect sizes, \hat{A}_{12} values of 0.56, 0.64, and 0.71 or higher correspond to small (S), medium (M), and large (L) effect sizes, respectively [47]. Given these thresholds, OPAL consistently demonstrates a large effect size on every dataset, indicating that it significantly outperforms all baselines for all datasets.

As shown in Figure 6, no single baseline consistently outperforms the others across all datasets. For instance, $B-VGG$ is the top-performer among the baselines for CIFAR-10, Fashion MNIST, and MNIST. However, it falls short compared to $B-Pseudo$ and $B-ResNet$ on other datasets. In contrast, OPAL surpasses all baselines across all datasets. Specifically, OPAL yields average accuracy improvements of 3.5%, 7.29%, 3.72%, and 3.5% over $B-VGG$, $B-ResNet$, $B-ViT$, and $B-Pseudo$, respectively, leading to an overall average improvement of 4.5% for all baselines and datasets.

Table V shows the average execution times for each step of OPAL and the baselines across all datasets. The data-splitting step has nearly identical execution times across the methods due to its identical implementation. OPAL requires more time for fine-tuning than the supervised baselines ($B-VGG$, $B-ResNet$, and $B-ViT$) as it fine-tunes three models instead of one. In contrast, $B-Pseudo$ is the most time-consuming among all methods, given its costly iterative fine-tuning process over the entire dataset. Finally, the MILP solver is very fast – significantly faster than fine-tuning, data splitting, and labelling. Since OPAL is executed offline rather than within a human feedback loop, its average runtime of approximately 15 minutes does not impede its practical applicability.

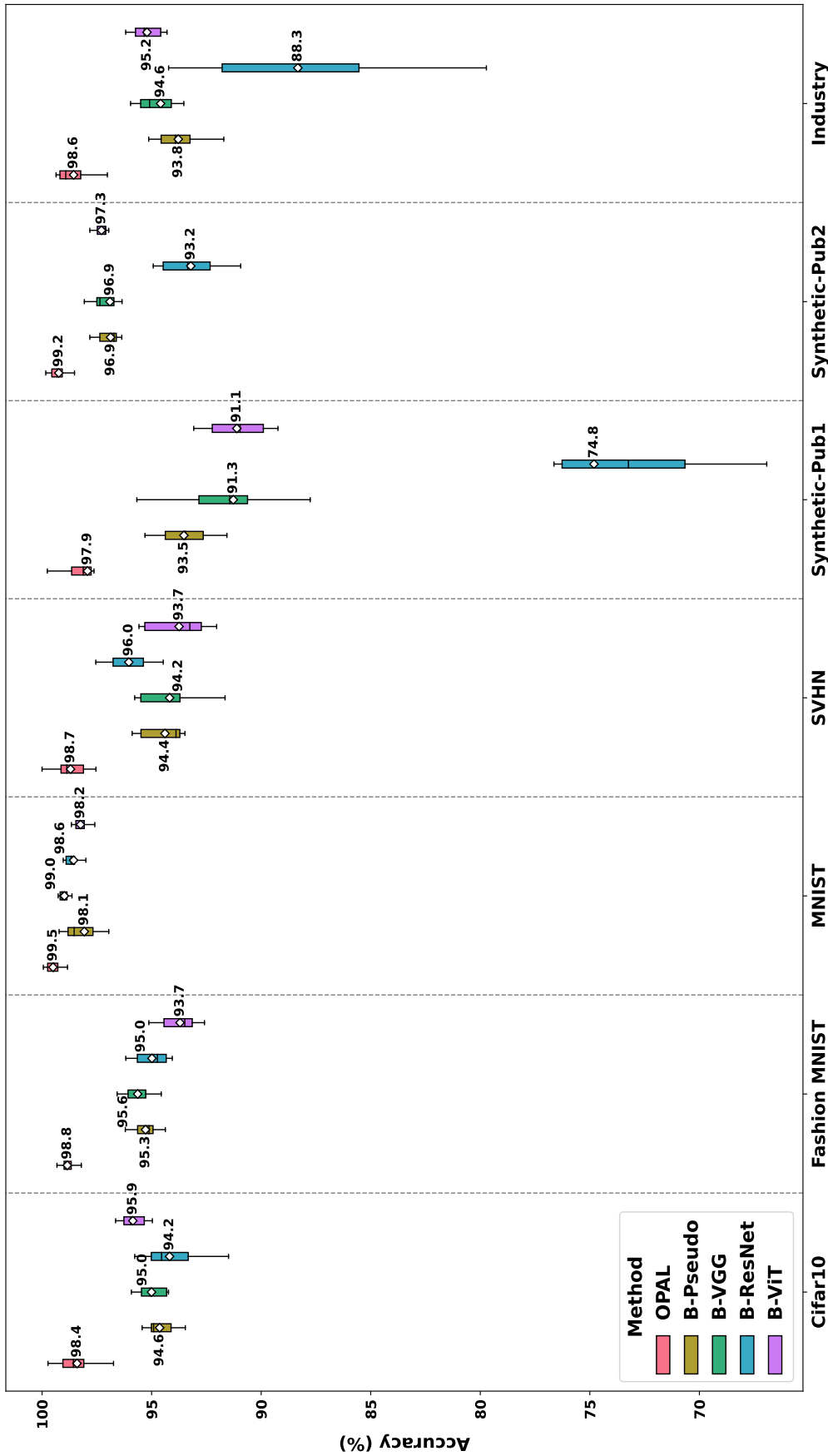


Fig. 6: Accuracy distributions obtained by OPAL and the baselines when all methods are provided with the same manual labelling effort that OPAL requires in RQ1 to achieve near-perfect accuracy.

TABLE V: Execution time of different steps for OPAL and baselines averaged over all datasets

Method	Execution Time (Seconds)				
	Data Splitting	Fine-Tuning	MILP Solver	Labelling	Total
OPAL	40.6 (4%)	785.9 (86%)	24.0 (3%)	62.9 (7%)	913.4
B-VGG	39.9 (11%)	281.3 (78%)	N/A	38.5 (11%)	359.7
B-ResNet	40.2 (12%)	247.8 (77%)	N/A	35.6 (11%)	323.6
B-ViT	43.0 (11%)	307.2 (78%)	N/A	42.7 (11%)	392.9
B-Pseudo	38.7 (2%)	2503.8 (98%)	N/A	N/A	2542.5

Finding: Across all seven datasets, and within the same manual labelling budget, OPAL achieves significantly higher labelling accuracy than all baseline methods, with large effect sizes.

Takeway: Under the same manual labelling effort required by OPAL in RQ1 to achieve an average near-perfect accuracy of 98.8%, none of the baselines can exceed an average accuracy of 95.3%. Further, OPAL’s execution time is feasible given its offline execution model.

RQ3 experiments. To answer RQ3, we first apply OPAL as presented in Algorithm 1 to the three test-input validation datasets: SYNTHETIC-PUB1, SYNTHETIC-PUB2, and INDUSTRY, and compare OPAL with the four test-input validation baselines described in Section V-A2. We then extend OPAL with an active-learning loop and repeat the same experiments. Below, we discuss experiments that compare OPAL and its active-learning variant against the test-input validation baselines.

Comparing OPAL with the test-input validation baselines in Section V-A2. For each of our four baselines for test-input validation, we experiment with three manual effort levels: 25%, 50% and 75%. More specifically, for B-VAE, B-VIF and B-HiL-TV1 when experimenting with $x\%$ manual effort, we initially train the baseline on a randomly selected $x\%$ of the input dataset. We then use the baseline to predict validation labels for the remaining $1-x\%$ of the dataset. For B-HiL-TV2, as suggested by the authors of that baseline [8], since it uses an active-learning loop, to experiment with $x\%$ manual effort, we initially train the baseline on $\frac{x}{2}\%$ of randomly selected data and then start the active-learning loop. Once the manual effort has reached $x\%$, we stop prompting the human in the loop and label the validity of the rest of the data automatically. We measure the accuracy and manual effort of each baseline similar to RQ1 and RQ2. To address randomness, like in RQ1, we repeat each experiment five times. In total, for the baselines, we perform $4(\text{baselines}) \times 3(\text{labelling budgets}) \times 3(\text{datasets}) \times 5(\text{repeats}) = 180$ experiments.

To run OPAL for test-input validation, we compute the 13 image-comparison metrics from Ghobari et al. [8] on each original-synthesized image pair. The resulting metrics produce a tabular dataset in which each row represents one image pair. Since DL models are generally ill-suited to tabular data [48], [49], Algorithm 1 uses a random-forest classifier, in line with Ghobari et al.’s finding that random forest outperforms other common classification techniques such as SVM, logistic regression, and decision trees for test-input validation.

For each baseline and effort level of 25%, 50%, and 75%, we apply OPAL to the SYNTHETIC-PUB1, SYNTHETIC-PUB2, and INDUSTRY datasets by setting the parameter α in Algorithm 1 to the average accuracy achieved by five runs of the baseline for that effort level and dataset. By doing so, we investigate how much effort OPAL requires to match or exceed the accuracies that baselines achieve for different effort levels. This approach allows us to experiment with and compare OPAL to baselines by setting α to a range of values, and to quantify how much manual effort OPAL saves compared to each baseline while matching or exceeding the baseline’s accuracy.

Comparing the active-learning variant of OPAL (OPAL-AL) with the test-input validation baselines. Algorithm 4 presents a variant of OPAL, referred to as OPAL-AL, which integrates active learning. The inputs and parameters of OPAL-AL are identical to those of Algorithm 1, except for the additional parameter β , which denotes the number of samples manually validated in each iteration of the active-learning loop. Similar to Algorithm 1, OPAL-AL starts by performing the data splitting routine (line 1 of Algorithm 4) and manually validating the fine-tuning dataset, D_t , and the optimization dataset, D_o (line 2 of Algorithm 4). Each iteration of the active-learning loop (lines 3–12 of Algorithm 4) starts by executing lines 3–16 of Algorithm 1 on sets D_t , D_o and D' , which is the to-be-labelled dataset. By doing so, OPAL’s MILP formulation automatically validates a subset of D' and identifies a subset D_m of D' that cannot be automatically validated with high accuracy. Instead of requesting manual validation for the entire D_m as done in OPAL, OPAL-AL randomly selects a subset of D_m with at most β elements and requests the human validator to validate this smaller subset (lines 5–7 of Algorithm 4). Then the sets D' , D_t and D_o are updated, by removing the manually validated elements from D' , and adding them to D_t and D_o (lines 8–11 of Algorithm 4). The active-learning loop of OPAL-AL continues until all of the elements in D' have been either automatically or manually validated.

For the parameters of OPAL-AL, we use the same configuration as that applied for comparing OPAL with the test-input-validation baselines. When comparing OPAL-AL with OPAL, the only new parameter is β . Ghobari et al. [8] showed that β affects only the number of iterations and has no significant impact on the accuracy or manual effort of test-input validation. We investigated OPAL-AL with β values of 10, 50, 100, and 150, which confirmed this observation. In the experimental results reported for RQ3, we use $\beta = 50$.

RQ3 Results. Tables VI, VII and VIII show the average accuracy (Acc) and average manual effort (ME) achieved by OPAL, OPAL-AL and the four baselines across our three test-input validation datasets: SYNTHETIC-PUB1, SYNTHETIC-PUB2, and INDUSTRY. For each of the four baselines – B-VAE, B-VIF, B-HiL-TV1, and B-HiL-TV2 – the results are presented for three human effort levels: 25%, 50%, and 75%. For each human effort level, we report the differences in accuracy (Δ_{Acc}) and manual effort (Δ_{ME}) between OPAL and each baseline, as well as between OPAL-AL and each baseline.

A positive Δ_{Acc} means OPAL (or OPAL-AL) outperforms the baseline. These values are highlighted green when OPAL’s

TABLE VI: Comparing OPAL and OPAL extended with active learning (i.e., OPAL-AL) with four test-input validation baselines described in Section V-A2 for SYNTHETIC-PUB1 dataset. For comparisons yielding a significance level of $p < 0.01$, the corresponding values of Δ_{ME} and Δ_{Acc} are emphasized in **boldface**. For manual effort and accuracy, if OPAL or OPAL-AL has outperformed a baseline, the corresponding Δ value is highlighted in green.

B-HiL-TV2		OPAL		OPAL vs B-HiL-TV2		OPAL-AL		OPAL-AL vs B-HiL-TV2	
ME	Acc	ME	Acc	Δ_{ME}	Δ_{Acc}	ME	Acc	Δ_{ME}	Δ_{Acc}
0.25	0.91	0.09	0.91	-0.16	0	0.18	0.92	-0.07	0.01
0.50	0.96	0.65	0.97	0.15	0.01	0.46	0.96	-0.04	0
0.75	0.99	0.81	0.99	0.06	0	0.56	0.97	-0.19	-0.02
B-HiL-TV1		OPAL		OPAL vs B-HiL-TV1		OPAL-AL		OPAL-AL vs B-HiL-TV1	
ME	Acc	ME	Acc	Δ_{ME}	Δ_{Acc}	ME	Acc	Δ_{ME}	Δ_{Acc}
0.25	0.86	0.09	0.9	-0.16	0.04	0.07	0.9	-0.18	0.04
0.50	0.87	0.09	0.9	-0.41	0.03	0.07	0.9	-0.43	0.03
0.75	0.88	0.07	0.89	-0.68	0.01	0.07	0.9	-0.68	0.02
B-VIF		OPAL		OPAL vs B-VIF		OPAL-AL		OPAL-AL vs B-VIF	
ME	Acc	ME	Acc	Δ_{ME}	Δ_{Acc}	ME	Acc	Δ_{ME}	Δ_{Acc}
0.25	0.81	0.08	0.89	-0.17	0.08	0.06	0.89	-0.19	0.08
0.50	0.81	0.08	0.89	-0.42	0.08	0.06	0.89	-0.44	0.08
0.75	0.81	0.08	0.89	-0.67	0.08	0.06	0.89	-0.69	0.08
B-VAE		OPAL		OPAL vs B-VAE		OPAL-AL		OPAL-AL vs B-VAE	
ME	Acc	ME	Acc	Δ_{ME}	Δ_{Acc}	ME	Acc	Δ_{ME}	Δ_{Acc}
0.25	0.81	0.08	0.89	-0.17	0.08	0.06	0.89	-0.19	0.08
0.50	0.81	0.08	0.89	-0.42	0.08	0.06	0.89	-0.44	0.08
0.75	0.81	0.08	0.89	-0.67	0.08	0.06	0.89	-0.69	0.08
Average								-0.352 (L)	0.047 (M)

Algorithm 4 OPAL with Active Learning (OPAL-AL)

Input D : An unlabelled dataset
Input α : Accuracy threshold
Input c_1, \dots, c_n : A set of pretrained classifiers
Param $h_{Initial}, s: \dots$
Param β : Maximum human validations per active-learning iteration // **The inputs, parameters, and output of OPAL-AL are the same as those of OPAL (Algorithm 1), except for the new β parameter.**
Output D : Labelled dataset

- 1: $(D_t, D_o, D') = \text{DataSplit}(D, h_{Initial}, s)$ // **Line 1 of Algorithm 1**
- 2: Manually validate $D_t \cup D_o$ // **Line 2 of Algorithm 1**
- 3: **while** $D' \neq \emptyset$ **do**
- 4: Execute lines 3 to 16 of OPAL (Algorithm 1) on D_t, D_o , and D'
- 5: $D' \leftarrow D_m$ // **D_m is the set of data to be manually validated as computed by the loop from lines 5–16 of Algorithm 1**
- 6: Randomly select $D_{imp} \subseteq D'$ with $|D_{imp}| = \min(\beta, |D'|)$
- 7: Prompt human to validate all pairs in D_{imp}
- 8: $D' \leftarrow D' \setminus D_{imp}$
- 9: Partition D_{imp} into two equal random splits $D_{imp,1}$ and $D_{imp,2}$.
- 10: $D_t \leftarrow D_t \cup D_{imp,1}$
- 11: $D_o \leftarrow D_o \cup D_{imp,2}$
- 12: **end while**
- 13: **return** D

accuracy (or OPAL-AL's accuracy) is equal to or higher than the baseline. Similarly, Δ_{ME} shows the difference in manual effort between OPAL (or OPAL-AL) and the baseline. A negative Δ_{ME} means OPAL (or OPAL-AL) outperforms the baseline and requires less effort. These values are highlighted green when OPAL's effort (or OPAL-AL's effort) is equal to or lower than the baseline. The last rows of Tables VI, VII and VIII show the average Δ_{Acc} and Δ_{ME} for our three test-input validation datasets. We conducted Wilcoxon rank-sum test and Vargha-Delaney \hat{A}_{12} test to compare accuracy and manual effort between the baselines and both OPAL and OPAL-AL.

For comparisons yielding a significance level of $p < 0.01$, the corresponding values of Δ_{ME} and Δ_{Acc} are emphasized in **boldface** in Tables VI, VII and VIII. Furthermore, the comparison results show a large effect size for manual effort reduction across all datasets when comparing OPAL and OPAL-AL with baselines, and medium to large effect sizes for accuracy improvements across all datasets when comparing OPAL and OPAL-AL with baselines.

As shown in Tables VI, VII and VIII, OPAL reduces manual effort by 31.0%, 24.0% and 31.5% and improves accuracy by 4.8%, 2.5% and 6.3% on the Synthetic-Pub1, Synthetic-Pub2 and Industry datasets, respectively. With active learning, OPAL-AL reduces manual effort by 35.2%, 28.0% and 37.0% while improving accuracy by 4.7%, 2.0% and 5.2% on the same datasets. Thus, adding the active-learning loop yields a further reduction in manual effort of 4.2%, 4.0% and 5.5% across the three datasets.

In 32 out of 36 cases, OPAL requires less manual effort than the baselines, while in 35 out of 36 cases, OPAL's accuracy is equal to or higher than the baselines. In all cases (36 out of 36), OPAL-AL requires less manual effort than the baselines, while in 30 out of 36 cases, OPAL-AL's accuracy is equal to or higher than the baselines.

Table IX reports the p-values from the Wilcoxon rank-sum test and the Vargha-Delaney \hat{A}_{12} effect sizes for validation accuracy and manual effort when comparing OPAL against OPAL-AL. Overall, on average, OPAL-AL requires 4.5% less effort compared to OPAL. We find that neither approach significantly outperforms the other in terms of validation accuracy. In contrast, OPAL-AL, significantly outperforms OPAL in terms of manual effort with medium and large effect

TABLE VII: Comparing OPAL and OPAL extended with active learning (i.e., OPAL-AL) with four test-input validation baselines described in Section V-A2 for SYNTHETIC-PUB2 dataset For comparisons yielding a significance level of $p < 0.01$, the corresponding values of Δ_{ME} and Δ_{Acc} are emphasized in **boldface**. For manual effort and accuracy, if OPAL or OPAL-AL has outperformed a baseline, the corresponding Δ value is highlighted in green.

B-HiL-TV2		OPAL		OPAL vs B-HiL-TV2		OPAL-AL		OPAL-AL vs B-HiL-TV2	
ME	Acc	ME	Acc	Δ_{ME}	Δ_{Acc}	ME	Acc	Δ_{ME}	Δ_{Acc}
0.25	0.9	0.19	0.91	-0.06	0.01	0.17	0.91	-0.08	0.01
0.50	0.92	0.26	0.94	-0.24	0.02	0.25	0.94	-0.25	0.02
0.75	0.97	0.42	0.97	-0.33	0	0.39	0.97	-0.36	0
B-HiL-TV1		OPAL		OPAL vs B-HiL-TV1		OPAL-AL		OPAL-AL vs B-HiL-TV1	
ME	Acc	ME	Acc	Δ_{ME}	Δ_{Acc}	ME	Acc	Δ_{ME}	Δ_{Acc}
0.25	0.88	0.14	0.88	-0.11	0	0.11	0.88	-0.14	0
0.50	0.89	0.24	0.93	-0.26	0.04	0.21	0.93	-0.29	0.04
0.75	0.96	0.39	0.96	-0.36	0	0.38	0.96	-0.37	0
B-VIF		OPAL		OPAL vs B-VIF		OPAL-AL		OPAL-AL vs B-VIF	
ME	Acc	ME	Acc	Δ_{ME}	Δ_{Acc}	ME	Acc	Δ_{ME}	Δ_{Acc}
0.25	0.86	0.13	0.87	-0.12	0.01	0.1	0.86	-0.15	0
0.50	0.86	0.24	0.93	-0.26	0.07	0.1	0.93	-0.4	0.07
0.75	0.95	0.39	0.95	-0.36	0	0.36	0.95	-0.39	0
B-VAE		OPAL		OPAL vs B-VAE		OPAL-AL		OPAL-AL vs B-VAE	
ME	Acc	ME	Acc	Δ_{ME}	Δ_{Acc}	ME	Acc	Δ_{ME}	Δ_{Acc}
0.25	0.82	0.11	0.87	-0.14	0.05	0.1	0.85	-0.15	0.03
0.50	0.83	0.24	0.93	-0.26	0.1	0.1	0.91	-0.4	0.08
0.75	0.95	0.39	0.95	-0.36	0	0.36	0.95	-0.39	0
Average				-0.24 (L)	0.025 (M)			-0.28 (L)	0.02 (M)

sizes. This shows that active learning loop can be considered as another factor to reduce manual effort.

Finding: Across all the three test-input validation datasets, on average, OPAL requires 28.8% less manual effort while achieving 4.5% higher accuracy compared to the four test-input validation baselines. Similarly, OPAL integrated with active learning, on average achieves 4% higher accuracy while reducing the manual effort 33.4% compared to the four test-input validation baselines.

Takeway: Extending OPAL with active learning improves its ability to further optimize the test-input validation effort by requiring an average of 4.5% less manual labeling effort compared to not using an active learning loop.

VII. THREATS TO VALIDITY

Internal validity. In our experiments, we ensure that OPAL and baselines are not fine-tuned on images that they will later label. Similarly, we prevent the MILP solver from processing images used during fine-tuning – which might otherwise yield artificially high confidence levels. Specifically, we address these concerns by maintaining separate, non-overlapping *fine-tuning*, *optimization*, and *to-be-labelled* subsets for each dataset throughout all experiments. Recognizing that potential biases may arise from dataset characteristics, we note that four of the seven datasets studied in this article – namely CIFAR10, FASHIONMNIST, MNIST and SVHN – are public benchmarks that are widely used by the research community. For these datasets, we directly used their existing labels as

ground truth. The ground-truth labels for SYNTHETIC-PUB1 and SYNTHETIC-PUB2 were adopted from Hu et al. [3]. The INDUSTRY dataset was independently labelled by two human annotators (who are not co-authors), with the final labels reviewed and verified by domain experts, as detailed in Section V-B.

To address the randomness associated with data splitting and the fine-tuning of classifiers in RQ1, RQ2 and RQ3, each experimental configuration was repeated five times. To avoid potential data leakage, we note that vision models allow full control over which pre-trained weights to use. In RQ1 and RQ2, the pre-trained weights for VGG, ResNet, and ViT – whether used in OPAL or the baselines – are exclusively based on ImageNet. None of the seven datasets studied overlap with ImageNet, eliminating potential data contamination. Therefore, OPAL and the baselines are not fine-tuned on images that they later label.

In RQ2, for a fair comparison of OPAL with the automated data-labelling baselines, OPAL and the baselines were evaluated using an equal amount of manual effort to investigate each method’s labelling accuracy. Similarly, in RQ3, fairness is ensured by comparing OPAL, with and without active learning, to baselines using the same accuracy targets as those achieved by the baselines.

External validity. Our experiments use seven diverse datasets and three state-of-the-art deep learning image classifiers. These datasets encompass a wide variety of images, including well-known benchmarks, real-world images, synthetic images, images of common-objects and industrial images. The three classifiers are based on deep learning architectures that have been extensively used across both research and industry [50]–[55]. The consistent results observed across

TABLE VIII: Comparing OPAL and OPAL extended with active learning (i.e., OPAL-AL) with four test-input validation baselines described in Section V-A2 for INDUSTRY dataset For comparisons yielding a significance level of $p < 0.01$, the corresponding values of Δ_{ME} and Δ_{Acc} are emphasized in **boldface**. For manual effort and accuracy, if OPAL or OPAL-AL has outperformed a baseline, the corresponding Δ value is highlighted in green.

B-HiL-TV2		OPAL		OPAL vs B-HiL-TV2		OPAL-AL		OPAL-AL vs B-HiL-TV2	
ME	Acc	ME	Acc	Δ_{ME}	Δ_{Acc}	ME	Acc	Δ_{ME}	Δ_{Acc}
0.25	0.97	0.32	0.97	0.07	0	0.11	0.94	-0.14	-0.03
0.50	0.99	0.46	0.98	-0.04	-0.01	0.33	0.97	-0.17	-0.02
0.75	1.00	0.81	1	0.06	0	0.63	1	-0.12	0
B-HiL-TV1		OPAL		OPAL vs B-HiL-TV1		OPAL-AL		OPAL-AL vs B-HiL-TV1	
ME	Acc	ME	Acc	Δ_{ME}	Δ_{Acc}	ME	Acc	Δ_{ME}	Δ_{Acc}
0.25	0.92	0.09	0.92	-0.16	0	0.06	0.91	-0.19	-0.01
0.50	0.92	0.09	0.92	-0.41	0	0.06	0.91	-0.44	-0.01
0.75	0.92	0.09	0.92	-0.66	0	0.06	0.91	-0.69	-0.01
B-VIF		OPAL		OPAL vs B-VIF		OPAL-AL		OPAL-AL vs B-VIF	
ME	Acc	ME	Acc	Δ_{ME}	Δ_{Acc}	ME	Acc	Δ_{ME}	Δ_{Acc}
0.25	0.88	0.05	0.91	-0.2	0.03	0.05	0.9	-0.2	0.02
0.50	0.89	0.08	0.91	-0.42	0.02	0.06	0.9	-0.44	0.01
0.75	0.89	0.08	0.91	-0.67	0.02	0.06	0.9	-0.69	0.01
B-VAE		OPAL		OPAL vs B-VAE		OPAL-AL		OPAL-AL vs B-VAE	
ME	Acc	ME	Acc	Δ_{ME}	Δ_{Acc}	ME	Acc	Δ_{ME}	Δ_{Acc}
0.25	0.68	0.05	0.91	-0.2	0.23	0.05	0.9	-0.2	0.22
0.50	0.68	0.05	0.91	-0.45	0.23	0.05	0.9	-0.45	0.22
0.75	0.68	0.05	0.91	-0.7	0.23	0.05	0.9	-0.7	0.22
Average								-0.37 (L)	0.052 (M)

TABLE IX: Wilcoxon rank-sum and Vargha-Delaney \hat{A}_{12} statistical tests between OPAL vs OPAL extended with active learning (i.e., OPAL-AL). For comparisons yielding a significance level of $p < 0.01$, the corresponding values of \hat{A}_{12} are emphasized in **boldface**

Dataset	P-value (Acc)	\hat{A}_{12} (Acc)	P-value (ME)	\hat{A}_{12} (ME)
Synthetic-Pub1	0.013	0.37 (M)	0.007	0.65(M)
Synthetic-Pub2	2.863×10^{-15}	0.48(S)	9.051×10^{-16}	0.96(L)
Industry	0.041	0.43 (M)	0.042	0.62(M)

different datasets provide strong evidence of our findings' generalizability. To further validate generalizability, our study can be replicated using other classifiers, such as DenseNet [56] and AlexNet [57], among others.

VIII. RELATED WORK

Within the machine learning community, several supervised [18]–[20] and semi-supervised [9], [11], [31], [58]–[60] methods have been proposed to effectively train classifiers on sparsely labelled datasets. Although these methods aim to maximize accuracy given an existing labelled dataset, they neither allow control over the desired accuracy threshold nor provide a mechanism to minimize labelling effort. As a result, they fail to use the available labelled data in an optimal way to reach the highest attainable accuracy. In our evaluation, for instance, when provided with the same amount of labelled data that enables OPAL to achieve an average accuracy of 98.8%, the baseline methods – including both supervised [18]–[20] and semi-supervised [9], [11] approaches – cannot exceed 95.3% average accuracy. Furthermore, supervised and semi-supervised learning often rely on a single classifier, whereas OPAL uses multiple classifiers. While one could theoretically

extend the baseline approaches to use multiple classifiers, any such extension would still need to address the problem of maximizing accuracy within a fixed labelling budget. To our knowledge, no prior work has used these baselines to develop an accuracy-driven, effort-optimized solution for data labelling. In contrast, OPAL employs MILP to achieve this goal both effectively and efficiently.

Approaches for testing vision systems include metamorphic testing, which modifies existing labelled images while preserving their original labels [3], [4], [7], [28], as well as prompt-based generative AI – such as Stable Diffusion [61] – which synthesizes images from textual prompts and heuristically derives labels from these prompts. However, both methods often produce images that either fail to preserve the intended labels or are unrecognizable to humans [2]–[4], [8], [62]. Recent studies classify such images as invalid test inputs, defining them as images that are under-represented in the training set of a given DL model, and suggest using out-of-distribution detection methods to identify them [2], [4], [63]. Specifically, DAIV [2] trains a VAE and uses its loss function to discriminate valid and invalid test inputs. Self-Oracle [63] uses auto-encoders and time-series-based anomaly detection to identify invalid test inputs for autonomous driving systems. Riccio and Tonella [4] have shown that automated test-input validators based on DAIV and Self-Oracle can achieve up to a 78% agreement rate with human validators. Hu et al. [3] propose to discriminate between valid and invalid test inputs using a metric based on VIF [33].

Ghobari et al. [8] introduce a test-input validation method based on active learning and using 13 image-comparison metrics, including VIF and the VAE loss function. These metrics were previously used to evaluate the effectiveness of

image-to-image translators in bridging the gap between simulated and real-world images for testing autonomous driving systems [32], [64]. Their work finds that both the use of active learning and the combination of multiple image-comparison metrics result in improvement over the baselines that rely exclusively on VIF or the VAE loss function. Yet, none of the above techniques are specifically designed to target a desired level of accuracy while minimizing human labelling effort. Our evaluation in Section V indicates that OPAL outperforms all the existing test-input validation methods we are aware of, namely the work of Ghobari et al. [8], Hu et al. [3] and Riccio and Tonella [4].

IX. CONCLUSION

We introduce OPAL, an accuracy-driven, effort-optimized data labelling and validation method that aims to meet a specified accuracy target with the least possible manual labelling effort. Through a mixed-integer linear programming formulation for optimization, OPAL achieves an average accuracy of 98.8% on seven diverse datasets while reducing manual labelling effort by more than half. OPAL significantly outperforms state-of-the-art baselines for test-data labelling and test-input validation. Further, we show that extending OPAL with active learning leads to an additional 4.5% reduction in manual labelling effort, without negatively impacting accuracy.

Existing data labelling and validation methods lack explicit control over the tolerance level for mislabelling; this can undermine reliable quality assurance of AI-enabled systems. OPAL addresses this limitation by introducing a risk-driven strategy that allows practitioners to specify their desired accuracy target, ensuring more reliable data labelling and validation based on the risk associated with incorrect labels or invalid data. This in turn helps ensure that labelling quality aligns with the specific application needs and analytical goals at hand.

X. CODE AND DATA AVAILABILITY

Our **replication package** including our code, the studied public datasets and the DL classifiers is available online [44].

REFERENCES

- [1] K. Pei, Y. Cao, J. Yang, and S. Jana, “Deepxplore: automated whitebox testing of deep learning systems,” *Communications of the ACM*, vol. 62, no. 11, pp. 137–145, 2019.
- [2] S. Dola, M. B. Dwyer, and M. L. Soffa, “Distribution-aware testing of neural networks using generative models,” in *43rd IEEE/ACM International Conference on Software Engineering, ICSE 2021, Madrid, Spain, 22-30 May 2021*. IEEE, 2021, pp. 226–237.
- [3] B. C. Hu, L. Marsso, K. Czarnecki, R. Salay, H. Shen, and M. Chechik, “If a human can see it, so should your system: Reliability requirements for machine vision components,” in *44th IEEE/ACM 44th International Conference on Software Engineering, ICSE 2022, Pittsburgh, PA, USA, May 25-27, 2022*. ACM, 2022, pp. 1145–1156.
- [4] V. Riccio and P. Tonella, “When and why test generators for deep learning produce invalid inputs: an empirical study,” in *2023 IEEE/ACM 45th International Conference on Software Engineering (ICSE)*. IEEE, 2023, pp. 1161–1173.
- [5] Y. Tian, K. Pei, S. Jana, and B. Ray, “Deeptest: automated testing of deep-neural-network-driven autonomous cars,” in *Proceedings of the 40th International Conference on Software Engineering, ICSE 2018, Gothenburg, Sweden, May 27 - June 03, 2018*, M. Chaudron, I. Crnkovic, M. Chechik, and M. Harman, Eds. ACM, 2018, pp. 303–314.
- [6] M. Zhang, Y. Zhang, L. Zhang, C. Liu, and S. Khurshid, “Deeproad: Gan-based metamorphic testing and input validation framework for autonomous driving systems,” in *Proceedings of the 33rd ACM/IEEE International Conference on Automated Software Engineering, ASE 2018, Montpellier, France, September 3-7, 2018*, M. Huchard, C. Kästner, and G. Fraser, Eds. ACM, 2018, pp. 132–142.
- [7] J. Guo, Y. Jiang, Y. Zhao, Q. Chen, and J. Sun, “Dlfuzz: differential fuzzing testing of deep learning systems,” in *Proceedings of the 2018 ACM Joint Meeting on European Software Engineering Conference and Symposium on the Foundations of Software Engineering, ESEC/SIGSOFT FSE 2018, Lake Buena Vista, FL, USA, November 04-09, 2018*. ACM, 2018, pp. 739–743.
- [8] D. Ghobari, M. H. Amini, D. Q. Tran, S. Park, S. Nejati, and M. Sabetzadeh, “Test input validation for vision-based dl systems: An active learning approach,” in *47th International Conference on Software Engineering (ICSE 2025)*, 2025, to appear. Available at <https://arxiv.org/abs/2501.01606>.
- [9] H. Pham, Z. Dai, Q. Xie, and Q. V. Le, “Meta pseudo labels,” in *Proceedings of the IEEE/CVF Conference on Computer Vision and Pattern Recognition (CVPR)*, June 2021, pp. 11 557–11 568.
- [10] T. Chen, S. Kornblith, M. Norouzi, and G. Hinton, “A simple framework for contrastive learning of visual representations,” in *Proceedings of the 37th International Conference on Machine Learning*, ser. ICML’20. JMLR.org, 2020.
- [11] D.-H. Lee et al., “Pseudo-label: The simple and efficient semi-supervised learning method for deep neural networks,” in *Workshop on challenges in representation learning, ICML*, vol. 3, no. 2. Atlanta, 2013, p. 896.
- [12] S. Duan, S. Chang, and J. C. Principe, “Labels, information, and computation: efficient learning using sufficient labels,” *Journal of Machine Learning Research*, vol. 24, Jan. 2023.
- [13] H. Song, M. Kim, D. Park, Y. Shin, and J.-G. Lee, “Learning from noisy labels with deep neural networks: A survey,” *IEEE Transactions on Neural Networks and Learning Systems*, vol. 34, no. 11, pp. 8135–8153, 2023.
- [14] C. G. Northcutt, A. Athalye, and J. Mueller, “Pervasive label errors in test sets destabilize machine learning benchmarks,” in *Proceedings of the Neural Information Processing Systems Track on Datasets and Benchmarks 1, NeurIPS Datasets and Benchmarks 2021, December 2021, virtual*, J. Vanschoren and S. Yeung, Eds., 2021. [Online]. Available: <https://arxiv.org/abs/2103.14749>
- [15] J. G. Adigun, M. Camilli, M. Felderer, A. Giusti, D. T. Matt, A. Perini, B. Russo, and A. Susi, “Collaborative artificial intelligence needs stronger assurances driven by risks,” *Computer*, vol. 55, no. 3, pp. 52–63, 2022.
- [16] S. P. Boyd and L. Vandenberghe, *Convex Optimization*. Cambridge University Press, 2014. [Online]. Available: <https://web.stanford.edu/~boyd/cvxbook/>
- [17] P. R. Thie and G. E. Keough, *An Introduction to Linear Programming and Game Theory*, 3rd ed. USA: Wiley-Interscience, 2008.
- [18] S. Liu and W. Deng, “Very deep convolutional neural network based image classification using small training sample size,” in *2015 3rd IAPR Asian Conference on Pattern Recognition (ACPR)*, 2015, pp. 730–734.
- [19] K. He, X. Zhang, S. Ren, and J. Sun, “Deep residual learning for image recognition,” in *Proceedings of the IEEE conference on computer vision and pattern recognition*, 2016, pp. 770–778.
- [20] A. Dosovitskiy, L. Beyer, A. Kolesnikov, D. Weissenborn, X. Zhai, T. Unterthiner, M. Dehghani, M. Minderer, G. Heigold, S. Gelly, J. Uszkoreit, and N. Houlsby, “An image is worth 16x16 words: Transformers for image recognition at scale,” in *9th International Conference on Learning Representations, ICLR 2021, Virtual Event, Austria, May 3-7, 2021*, 2021.
- [21] O. Russakovsky, J. Deng, H. Su, J. Krause, S. Satheesh, S. Ma, Z. Huang, A. Karpathy, A. Khosla, M. Bernstein, A. C. Berg, and L. Fei-Fei, “ImageNet Large Scale Visual Recognition Challenge,” *International Journal of Computer Vision (IJCV)*, vol. 115, no. 3, pp. 211–252, 2015.
- [22] S. Luke, *Essentials of Metaheuristics*, 2nd ed. Lulu, 2013, available for free at <http://cs.gmu.edu/~sean/book/metaheuristics/>.
- [23] S. Mitchell, M. O’Sullivan, and I. Dunning, “Pulp: a linear programming toolkit for python,” *The University of Auckland, Auckland, New Zealand*, vol. 65, p. 25, 2011.
- [24] D. Ha and D. Eck, “A neural representation of sketch drawings,” in *6th International Conference on Learning Representations, ICLR 2018, Vancouver, BC, Canada, April 30 - May 3, 2018, Conference Track Proceedings*, 2018.

- [25] O. Berman and N. Ashrafi, "Optimization models for reliability of modular software systems," *IEEE Transactions on Software Engineering*, vol. 19, no. 11, pp. 1119–1123, Nov 1993.
- [26] G. Ruhe, "Optimization in Software Engineering: A Pragmatic Approach," in *Contemporary Empirical Methods in Software Engineering*, M. Felderer and G. Travassos, Eds. Springer, Cham, 2020.
- [27] C. Henard, M. Papadakis, M. Harman, and Y. Le Traon, "Combining Multi-Objective Search and Constraint Solving for Configuring Large Software Product Lines," in *Proceedings of the 37th IEEE/ACM International Conference on Software Engineering*, Florence, Italy, 2015, pp. 517–528.
- [28] P. Arcaini, A. Bombarda, S. Bonfanti, and A. Gargantini, "Dealing with robustness of convolutional neural networks for image classification," in *IEEE International Conference On Artificial Intelligence Testing, AITest 2020*, 2020, pp. 7–14.
- [29] T. Brooks, A. Holynski, and A. A. Efros, "Instructpix2pix: Learning to follow image editing instructions," in *IEEE/CVF Conference on Computer Vision and Pattern Recognition, CVPR 2023, Vancouver, BC, Canada, June 17-24, 2023*. IEEE, 2023, pp. 18 392–18 402.
- [30] B. Settles, "Active learning literature survey," University of Wisconsin–Madison, Tech. Rep., 2009.
- [31] K. Sohn, D. Berthelot, N. Carlini, Z. Zhang, H. Zhang, C. Raffel, E. D. Cubuk, A. Kurakin, and C. Li, "Fixmatch: Simplifying semi-supervised learning with consistency and confidence," in *Advances in Neural Information Processing Systems 33: Annual Conference on Neural Information Processing Systems 2020, NeurIPS 2020, December 6-12, 2020, virtual*, H. Larochelle, M. Ranzato, R. Hadsell, M. Balcan, and H. Lin, Eds., 2020.
- [32] S. C. Lambertenghi and A. Stocco, "Assessing quality metrics for neural reality gap input mitigation in autonomous driving testing," in *IEEE Conference on Software Testing, Verification and Validation, ICST 2024, Toronto, ON, Canada, May 27-31, 2024*. IEEE, 2024, pp. 173–184.
- [33] H. R. Sheikh and A. C. Bovik, "Image information and visual quality," *IEEE Transactions on image processing*, vol. 15, no. 2, pp. 430–444, 2006.
- [34] A. Krizhevsky, "Learning multiple layers of features from tiny images," University of Toronto, Tech. Rep., 2009.
- [35] H. Xiao, K. Rasul, and R. Vollgraf, "Fashion-mnist: a novel image dataset for benchmarking machine learning algorithms," *arXiv preprint arXiv:1708.07747*, 2017.
- [36] Y. LeCun, L. Bottou, Y. Bengio, and P. Haffner, "Gradient-based learning applied to document recognition," *Proceedings of the IEEE*, vol. 86, no. 11, pp. 2278–2324, 1998.
- [37] Y. Netzer, T. Wang, A. Coates, A. Bissacco, B. Wu, and A. Y. Ng, "Reading digits in natural images with unsupervised feature learning," *NIPS Workshop on Deep Learning and Unsupervised Feature Learning*, 2011.
- [38] A. Buslaev, V. I. Iglovikov, E. Khvedchenya, A. Parinov, M. Druzhinin, and A. A. Kalinin, "Albumentations: Fast and flexible image augmentations," *Information*, vol. 11, no. 2, p. 125, 2020.
- [39] C. Arora, M. Sabetzadeh, S. Nejati, and L. C. Briand, "An active learning approach for improving the accuracy of automated domain model extraction," *ACM Transactions on Software Engineering and Methodology*, vol. 28, no. 1, pp. 4:1–4:34, 2019.
- [40] A. Paszke, S. Gross, F. Massa, A. Lerer, J. Bradbury, G. Chanan, T. Killeen, Z. Lin, N. Gimelshein, L. Antiga, A. Desmaison, A. Kopf, E. Yang, Z. DeVito, M. Raison, A. Tejani, S. Chilamkurthy, B. Steiner, L. Fang, J. Bai, and S. Chintala, "Pytorch: An imperative style, high-performance deep learning library," pp. 8024–8035, 2019.
- [41] F. Pedregosa, G. Varoquaux, A. Gramfort, V. Michel, B. Thirion, O. Grisel, M. Blondel, P. Prettenhofer, R. Weiss, V. Dubourg, J. Vanderplas, A. Passos, D. Cournapeau, M. Brucher, M. Perrot, and E. Duchesnay, "Scikit-learn: Machine learning in Python," *Journal of Machine Learning Research*, vol. 12, pp. 2825–2830, 2011.
- [42] M. Ester, H.-P. Kriegel, J. Sander, and X. Xu, "A density-based algorithm for discovering clusters in large spatial databases with noise," in *Proceedings of the Second International Conference on Knowledge Discovery and Data Mining*, 1996, p. 226–231.
- [43] J. Han, M. Kamber, and J. Pei, *Data Mining: Concepts and Techniques*, 3rd ed. San Francisco, CA: Morgan Kaufmann, 2011.
- [44] "Replication package (OPAL)," <https://github.com/M-H-Amini/MILP>, 2025, [Online; accessed July 8, 2025].
- [45] I. Goodfellow, Y. Bengio, and A. Courville, *Deep Learning*. MIT Press, 2016, <http://www.deeplearningbook.org>.
- [46] D. Rey and M. Neuhäuser, *Wilcoxon-Signed-Rank Test*. Springer Berlin Heidelberg, 2011.
- [47] A. Vargha and H. D. Delaney, "A critique and improvement of the cl common language effect size statistics of mcgraw and wong," *Journal of Educational and Behavioral Statistics*, vol. 25, no. 2, pp. 101–132, 2000.
- [48] R. Shwartz-Ziv and A. Armon, "Tabular data: Deep learning is not all you need," *Information Fusion*, vol. 81, pp. 84–90, 2022.
- [49] L. Grinsztajn, E. Oyallon, and G. Varoquaux, "Why do tree-based models still outperform deep learning on typical tabular data?" in *Datasets and Benchmarks Track, Thirty-sixth Conference on Neural Information Processing Systems (NeurIPS 2022)*, 2022.
- [50] H. Touvron, M. Cord, M. Douze, F. Massa, A. Sablayrolles, and H. Jégou, "Training data-efficient image transformers & distillation through attention," in *Proceedings of the IEEE/CVF International Conference on Computer Vision*, 2021, pp. 538–547.
- [51] L. Wang, Y. Xiong, Z. Wang, Y. Qiao, D. Lin, X. Tang, and L. Van Gool, "Temporal segment networks: Towards good practices for deep action recognition," in *European Conference on Computer Vision*, 2016, pp. 20–36.
- [52] R. Girshick, "Fast r-cnn," in *Proceedings of the IEEE International Conference on Computer Vision*, 2015, pp. 1440–1448.
- [53] G. Boesch, "Deep residual networks (resnet, resnet-50)," *Viso.ai*, 2023.
- [54] O. M. Parkhi, A. Vedaldi, and A. Zisserman, "Deep face recognition," *British Machine Vision Conference (BMVC)*, 2015.
- [55] A. Radford, J. W. Kim, C. Hallacy, A. Ramesh *et al.*, "Learning transferable visual models from natural language supervision," *International Conference on Machine Learning (ICML)*, 2021.
- [56] G. Huang, Z. Liu, L. Van Der Maaten, and K. Q. Weinberger, "Densely connected convolutional networks," in *2017 IEEE Conference on Computer Vision and Pattern Recognition (CVPR)*, 2017, pp. 2261–2269.
- [57] A. Krizhevsky, I. Sutskever, and G. E. Hinton, "Imagenet classification with deep convolutional neural networks," in *Advances in Neural Information Processing Systems*, vol. 25, 2012.
- [58] S. Laine and T. Aila, "Temporal ensembling for semi-supervised learning," in *International Conference on Learning Representations (ICLR)*, 2017.
- [59] M. Sajjadi, M. Javanmardi, and T. Tasdizen, "Regularization with stochastic transformations and perturbations for deep semi-supervised learning," in *Advances in Neural Information Processing Systems (NeurIPS)*, 2016.
- [60] D. Berthelot, N. Carlini, I. Goodfellow, N. Papernot, A. Oliver, and C. Raffel, "Mixmatch: A holistic approach to semi-supervised learning," in *Advances in Neural Information Processing Systems (NeurIPS)*, 2019. [Online]. Available: <https://arxiv.org/abs/1905.02249>
- [61] P. Esser, S. Kulal, A. Blattmann, R. Entezari, J. Müller, H. Saini, Y. Levi, D. Lorenz, A. Sauer, F. Boesel *et al.*, "Scaling rectified flow transformers for high-resolution image synthesis," in *Forty-first International Conference on Machine Learning*, 2024.
- [62] V. Riccio, G. Jahangirova, A. Stocco, N. Humbatova, M. Weiss, and P. Tonella, "Testing machine learning based systems: a systematic mapping," *Empir. Softw. Eng.*, vol. 25, no. 6, pp. 5193–5254, 2020.
- [63] A. Stocco, M. Weiss, M. Calzana, and P. Tonella, "Misbehaviour prediction for autonomous driving systems," in *ICSE '20: 42nd International Conference on Software Engineering, Seoul, South Korea, 27 June - 19 July, 2020*, G. Rothermel and D. Bae, Eds. ACM, 2020, pp. 359–371.
- [64] M. H. Amini and S. Nejati, "Bridging the gap between real-world and synthetic images for testing autonomous driving systems," in *Proceedings of the 39th IEEE/ACM International Conference on Automated Software Engineering, ASE 2024, Sacramento, CA, USA, October 27 - November 1, 2024*, V. Filkov, B. Ray, and M. Zhou, Eds. ACM, 2024, pp. 732–744.